Draft version August 16, 2019
Typeset using LaTeX **twocolumn** style in AASTeX62

A gravitational-wave measurement of the Hubble constant following the second observing run of Advanced LIGO and Virgo

B. P. Abbott,[1] R. Abbott,[1] T. D. Abbott,[2] S. Abraham,[3] F. Acernese,[4,5] K. Ackley,[6] C. Adams,[7] R. X. Adhikari,[1] V. B. Adya,[8] C. Affeldt,[9,10] M. Agathos,[11,12] K. Agatsuma,[13] N. Aggarwal,[14] O. D. Aguiar,[15] L. Aiello,[16,17] A. Ain,[3] P. Ajith,[18] G. Allen,[19] A. Allocca,[20,21] M. A. Aloy,[22] P. A. Altin,[8] A. Amato,[23] S. Anand,[1] A. Ananyeva,[1] S. B. Anderson,[1] W. G. Anderson,[24] S. V. Angelova,[25] S. Antier,[26] S. Appert,[1] K. Arai,[1] M. C. Araya,[1] J. S. Areeda,[27] M. Arène,[26] N. Arnaud,[28,29] S. M. Aronson,[30] K. G. Arun,[31] S. Ascenzi,[16,32] G. Ashton,[6] S. M. Aston,[7] P. Astone,[33] F. Aubin,[34] P. Aufmuth,[10] K. AultONeal,[35] C. Austin,[2] V. Avendano,[36] A. Avila-Alvarez,[27] S. Babak,[26] P. Bacon,[26] F. Badaracco,[16,17] M. K. M. Bader,[37] S. Bae,[38] J. Baird,[26] P. T. Baker,[39] F. Baldaccini,[40,41] G. Ballardin,[29] S. W. Ballmer,[42] A. Bals,[35] S. Banagiri,[43] J. C. Barayoga,[1] C. Barbieri,[44,45] S. E. Barclay,[46] B. C. Barish,[1] D. Barker,[47] K. Barkett,[48] S. Barnum,[14] F. Barone,[49,5] B. Barr,[46] L. Barsotti,[14] M. Barsuglia,[26] D. Barta,[50] J. Bartlett,[47] I. Bartos,[30] R. Bassiri,[51] A. Basti,[20,21] M. Bawaj,[52,41] J. C. Bayley,[46] M. Bazzan,[53,54] B. Bécsy,[55] M. Bejger,[26,56] I. Belahcene,[28] A. S. Bell,[46] D. Beniwal,[57] M. G. Benjamin,[35] B. K. Berger,[51] G. Bergmann,[9,10] S. Bernuzzi,[11] C. P. L. Berry,[58] D. Bersanetti,[59] A. Bertolini,[37] J. Betzwieser,[7] R. Bhandare,[60] J. Bidler,[27] E. Biggs,[24] I. A. Bilenko,[61] S. A. Bilgili,[39] G. Billingsley,[1] R. Birney,[25] O. Birnholtz,[62] S. Biscans,[1,14] M. Bischi,[63,64] S. Biscoveanu,[14] A. Bisht,[10] M. Bitossi,[29,21] M. A. Bizouard,[65] J. K. Blackburn,[1] J. Blackman,[48] C. D. Blair,[7] D. G. Blair,[66] R. M. Blair,[47] S. Bloemen,[67] F. Bobba,[68,69] N. Bode,[9,10] M. Boer,[65] Y. Boetzel,[70] G. Bogaert,[65] F. Bondu,[71] R. Bonnand,[34] P. Booker,[9,10] B. A. Boom,[37] R. Bork,[1] V. Boschi,[29] S. Bose,[3] V. Bossilkov,[66] J. Bosveld,[66] Y. Bouffanais,[53,54] A. Bozzi,[29] C. Bradaschia,[21] P. R. Brady,[24] A. Bramley,[7] M. Branchesi,[16,17] J. E. Brau,[72] M. Breschi,[11] T. Briant,[73] J. H. Briggs,[46] F. Brighenti,[63,64] A. Brillet,[65] M. Brinkmann,[9,10] P. Brockill,[24] A. F. Brooks,[1] J. Brooks,[29] D. D. Brown,[57] S. Brunett,[1] A. Buikema,[14] T. Bulik,[74] H. J. Bulten,[75,37] A. Buonanno,[76,77] D. Buskulic,[34] C. Buy,[26] R. L. Byer,[51] M. Cabero,[9,10] L. Cadonati,[78] G. Cagnoli,[79] C. Cahillane,[1] J. Calderón Bustillo,[6] T. A. Callister,[1] E. Calloni,[80,5] J. B. Camp,[81] W. A. Campbell,[6] M. Canepa,[82,59] K. C. Cannon,[83] H. Cao,[57] J. Cao,[84] G. Carapella,[68,69] F. Carbognani,[29] S. Caride,[85] M. F. Carney,[58] G. Carullo,[20,21] J. Casanueva Diaz,[21] C. Casentini,[86,32] S. Caudill,[37] M. Cavaglià,[87,88] F. Cavalier,[28] R. Cavalieri,[29] G. Cella,[21] P. Cerdá-Durán,[22] E. Cesarini,[89,32] O. Chaibi,[65] K. Chakravarti,[3] S. J. Chamberlin,[90] M. Chan,[46] S. Chao,[91] P. Charlton,[92] E. A. Chase,[58] E. Chassande-Mottin,[26] D. Chatterjee,[24] M. Chaturvedi,[60] B. D. Cheeseboro,[39] H. Y. Chen,[93] X. Chen,[66] Y. Chen,[48] H.-P. Cheng,[30] C. K. Cheong,[94] H. Y. Chia,[30] F. Chiadini,[95,69] A. Chincarini,[59] A. Chiummo,[29] G. Cho,[96] H. S. Cho,[97] M. Cho,[77] N. Christensen,[98,65] Q. Chu,[66] S. Chua,[73] K. W. Chung,[94] S. Chung,[66] G. Ciani,[53,54] M. Cieślar,[56] A. A. Ciobanu,[57] R. Ciolfi,[99,54] F. Cipriano,[65] A. Cirone,[82,59] F. Clara,[47] J. A. Clark,[78] P. Clearwater,[100] F. Cleva,[65] E. Coccia,[16,17] P.-F. Cohadon,[73] D. Cohen,[28] M. Colleoni,[101] C. G. Collette,[102] C. Collins,[13] M. Colpi,[44,45] L. R. Cominsky,[103] M. Constancio Jr.,[15] L. Conti,[54] S. J. Cooper,[13] P. Corban,[7] T. R. Corbitt,[2] I. Cordero-Carrión,[104] S. Corezzi,[40,41] K. R. Corley,[105] N. Cornish,[55] D. Corre,[28] A. Corsi,[85] S. Cortese,[29] C. A. Costa,[15] R. Cotesta,[76] M. W. Coughlin,[1] S. B. Coughlin,[106,58] J.-P. Coulon,[65] S. T. Countryman,[105] P. Couvares,[1] P. B. Covas,[101] E. E. Cowan,[78] D. M. Coward,[66] M. J. Cowart,[7] D. C. Coyne,[1] R. Coyne,[107] J. D. E. Creighton,[24] T. D. Creighton,[108] J. Cripe,[2] M. Croquette,[73] S. G. Crowder,[109] T. J. Cullen,[2] A. Cumming,[46] L. Cunningham,[46] E. Cuoco,[29] T. Dal Canton,[81] G. Dálya,[110] B. D'Angelo,[82,59] S. L. Danilishin,[9,10] S. D'Antonio,[32] K. Danzmann,[10,9] A. Dasgupta,[111] C. F. Da Silva Costa,[30] L. E. H. Datrier,[46] V. Dattilo,[29] I. Dave,[60] M. Davier,[28] D. Davis,[42] E. J. Daw,[112] D. DeBra,[51] M. Deenadayalan,[3] J. Degallaix,[23] M. De Laurentis,[80,5] S. Deléglise,[73] W. Del Pozzo,[20,21] L. M. DeMarchi,[58] N. Demos,[14] T. Dent,[113] R. De Pietri,[114,115] R. De Rosa,[80,5] C. De Rossi,[23,29] R. DeSalvo,[116] O. de Varona,[9,10] S. Dhurandhar,[3] M. C. Díaz,[108] T. Dietrich,[37] L. Di Fiore,[5] C. DiFronzo,[13] C. Di Giorgio,[68,69] F. Di Giovanni,[22] M. Di Giovanni,[117,118] T. Di Girolamo,[80,5] A. Di Lieto,[20,21] B. Ding,[102] S. Di Pace,[119,33] I. Di Palma,[119,33] F. Di Renzo,[20,21] A. K. Divakarla,[30] A. Dmitriev,[13] Z. Doctor,[93] F. Donovan,[14] K. L. Dooley,[106,87] S. Doravari,[3] I. Dorrington,[106] T. P. Downes,[24] M. Drago,[16,17] J. C. Driggers,[47] Z. Du,[84] J.-G. Ducoin,[28] P. Dupej,[46] O. Durante,[68,69] S. E. Dwyer,[47] P. J. Easter,[6] G. Eddolls,[46] T. B. Edo,[112] A. Effler,[7] P. Ehrens,[1] J. Eichholz,[8] S. S. Eikenberry,[30] M. Eisenmann,[34] R. A. Eisenstein,[14] L. Errico,[80,5] R. C. Essick,[93] H. Estelles,[101] D. Estevez,[34] Z. B. Etienne,[39] T. Etzel,[1] M. Evans,[14] T. M. Evans,[7] V. Fafone,[86,32,16] S. Fairhurst,[106] X. Fan,[84] S. Farinon,[59] B. Farr,[72] W. M. Farr,[13] E. J. Fauchon-Jones,[106] M. Favata,[36] M. Fays,[112] M. Fazio,[120] C. Fee,[121] J. Feicht,[1] M. M. Fejer,[51] F. Feng,[26] A. Fernandez-Galiana,[14] I. Ferrante,[20,21] E. C. Ferreira,[15] T. A. Ferreira,[15] F. Fidecaro,[20,21] I. Fiori,[29] D. Fiorucci,[16,17] M. Fishbach,[93] R. P. Fisher,[122] J. M. Fishner,[14] R. Fittipaldi,[123,69] M. Fitz-Axen,[43] V. Fiumara,[124,69] R. Flaminio,[34,125] M. Fletcher,[46] E. Floden,[43] E. Flynn,[27] H. Fong,[83] J. A. Font,[22,126] P. W. F. Forsyth,[8] J.-D. Fournier,[65] Francisco Hernandez Vivanco,[6] S. Frasca,[119,33] F. Frasconi,[21] Z. Frei,[110] A. Freise,[13] R. Frey,[72] V. Frey,[28] P. Fritschel,[14] V. V. Frolov,[7] G. Fronzè,[127] P. Fulda,[30] M. Fyffe,[7] H. A. Gabbard,[46] B. U. Gadre,[76] S. M. Gaebel,[13] J. R. Gair,[128] L. Gammaitoni,[40] S. G. Gaonkar,[3] C. García-Quirós,[101] F. Garufi,[80,5] B. Gateley,[47] S. Gaudio,[35] G. Gaur,[129] V. Gayathri,[130] G. Gemme,[59] E. Genin,[29] A. Gennai,[21] D. George,[19] J. George,[60] L. Gergely,[131] S. Ghonge,[78] Abhirup Ghosh,[76] Archisman Ghosh,[37] S. Ghosh,[24] B. Giacomazzo,[117,118] J. A. Giaime,[2,7] K. D. Giardina,[7] D. R. Gibson,[132] K. Gill,[105] L. Glover,[133] J. Gniesmer,[134] P. Godwin,[90] E. Goetz,[47] R. Goetz,[30] B. Goncharov,[6] G. González,[2] J. M. Gonzalez Castro,[20,21] A. Gopakumar,[135] S. E. Gossan,[1] M. Gosselin,[29,20,21] R. Gouaty,[34] B. Grace,[8] A. Grado,[136,5] M. Granata,[23] A. Grant,[46] S. Gras,[14] P. Grassia,[1] C. Gray,[47] R. Gray,[46] G. Greco,[63,64] A. C. Green,[30] R. Green,[106] E. M. Gretarsson,[35] A. Grimaldi,[117,118] S. J. Grimm,[16,17] P. Groot,[67] H. Grote,[106] S. Grunewald,[76] P. Gruning,[28] G. M. Guidi,[63,64] H. K. Gulati,[111] Y. Guo,[37] A. Gupta,[90] Anchal Gupta,[1] P. Gupta,[37] E. K. Gustafson,[1] R. Gustafson,[137] L. Haegel,[101] O. Halim,[17,16] B. R. Hall,[138] E. D. Hall,[14] E. Z. Hamilton,[106] G. Hammond,[46] M. Haney,[70] M. M. Hanke,[9,10] J. Hanks,[47] C. Hanna,[90] M. D. Hannam,[106] O. A. Hannuksela,[94] T. J. Hansen,[35] J. Hanson,[7] T. Harder,[65] T. Hardwick,[2] K. Haris,[18] J. Harms,[16,17] G. M. Harry,[139] I. W. Harry,[140] R. K. Hasskew,[7] C. J. Haster,[14] K. Haughian,[46] F. J. Hayes,[46] J. Healy,[62] A. Heidmann,[73] M. C. Heintze,[7] H. Heitmann,[65] F. Hellman,[141] P. Hello,[28] G. Hemming,[29] M. Hendry,[46] I. S. Heng,[46] J. Hennig,[9,10] M. Heurs,[9,10] S. Hild,[46] T. Hinderer,[142,37,143] S. Hochheim,[9,10] D. Hofman,[23] A. M. Holgado,[19] N. A. Holland,[8] K. Holt,[7] D. E. Holz,[93] P. Hopkins,[106] C. Horst,[24] J. Hough,[46] E. J. Howell,[66] C. G. Hoy,[106] Y. Huang,[14] M. T. Hübner,[6] E. A. Huerta,[19] D. Huet,[28] B. Hughey,[35] V. Hui,[34] S. Husa,[101] S. H. Huttner,[46] T. Huynh-Dinh,[7] B. Idzkowski,[74] A. Iess,[86,32] H. Inchauspe,[30] C. Ingram,[57] R. Inta,[85] G. Intini,[119,33] B. Irwin,[121] H. N. Isa,[46] J.-M. Isac,[73] M. Isi,[14] B. R. Iyer,[18] T. Jacqmin,[73] S. J. Jadhav,[144] K. Jani,[78] N. N. Janthalur,[144] P. Jaranowski,[145] D. Jariwala,[30] A. C. Jenkins,[146] J. Jiang,[30] D. S. Johnson,[19] A. W. Jones,[13] D. I. Jones,[147] J. D. Jones,[47] R. Jones,[46] R. J. G. Jonker,[37] L. Ju,[66] J. Junker,[9,10] C. V. Kalaghatgi,[106] V. Kalogera,[58] B. Kamai,[1] S. Kandhasamy,[3] G. Kang,[38] J. B. Kanner,[1] S. J. Kapadia,[24] S. Karki,[72] R. Kashyap,[18] M. Kasprzack,[1] S. Katsanevas,[29] E. Katsavounidis,[14] W. Katzman,[7] S. Kaufer,[10] K. Kawabe,[47] N. V. Keerthana,[3] F. Kéfélian,[65] D. Keitel,[140] R. Kennedy,[112] J. S. Key,[148] F. Y. Khalili,[61]

I. Khan,[16,32] S. Khan,[9,10] E. A. Khazanov,[149] N. Khetan,[16,17] M. Khursheed,[60] N. Kijbunchoo,[8] Chunglee Kim,[150] J. C. Kim,[151] K. Kim,[94] W. Kim,[57] W. S. Kim,[152] Y.-M. Kim,[153] C. Kimball,[58] P. J. King,[47] M. Kinley-Hanlon,[46] R. Kirchhoff,[9,10] J. S. Kissel,[47] L. Kleybolte,[134] J. H. Klika,[24] S. Klimenko,[30] T. D. Knowles,[39] P. Koch,[9,10] S. M. Koehlenbeck,[9,10] G. Koekoek,[37,154] S. Koley,[37] V. Kondrashov,[1] A. Kontos,[155] N. Koper,[9,10] M. Korobko,[134] W. Z. Korth,[1] M. Kovalam,[66] D. B. Kozak,[1] C. Krämer,[9,10] V. Kringel,[9,10] N. Krishnendu,[31] A. Królak,[156,157] N. Krupinski,[24] G. Kuehn,[9,10] A. Kumar,[144] P. Kumar,[158] Rahul Kumar,[47] Rakesh Kumar,[111] L. Kuo,[91] A. Kutynia,[156] S. Kwang,[24] B. D. Lackey,[76] D. Laghi,[20,21] K. H. Lai,[94] T. L. Lam,[94] M. Landry,[47] B. B. Lane,[14] R. N. Lang,[159] J. Lange,[62] B. Lantz,[51] R. K. Lanza,[14] A. Lartaux-Vollard,[28] P. D. Lasky,[6] M. Laxen,[7] A. Lazzarini,[1] C. Lazzaro,[54] P. Leaci,[119,33] S. Leavey,[9,10] Y. K. Lecoeuche,[47] C. H. Lee,[97] H. K. Lee,[160] H. M. Lee,[161] H. W. Lee,[151] J. Lee,[96] K. Lee,[46] J. Lehmann,[9,10] A. K. Lenon,[39] N. Leroy,[28] N. Letendre,[34] Y. Levin,[6] A. Li,[94] J. Li,[84] K. J. L. Li,[94] T. G. F. Li,[94] X. Li,[48] F. Lin,[6] F. Linde,[162,37] S. D. Linker,[133] T. B. Littenberg,[163] J. Liu,[66] X. Liu,[24] M. Llorens-Monteagudo,[22] R. K. L. Lo,[94,1] L. T. London,[14] A. Longo,[164,165] M. Lorenzini,[16,17] V. Loriette,[166] M. Lormand,[7] G. Losurdo,[21] J. D. Lough,[9,10] C. O. Lousto,[62] G. Lovelace,[27] M. E. Lower,[167] H. Lück,[10,9] D. Lumaca,[86,32] A. P. Lundgren,[140] R. Lynch,[14] Y. Ma,[48] R. Macas,[106] S. Macfoy,[25] M. MacInnis,[14] D. M. Macleod,[106] A. Macquet,[65] I. Magaña Hernandez,[24] F. Magaña-Sandoval,[30] R. M. Magee,[90] E. Majorana,[33] I. Maksimovic,[166] A. Malik,[60] N. Man,[65] V. Mandic,[43] V. Mangano,[46,119,33] G. L. Mansell,[47,14] M. Manske,[24] M. Mantovani,[29] M. Mapelli,[53,54] F. Marchesoni,[52,41] F. Marion,[34] S. Márka,[105] Z. Márka,[105] C. Markakis,[19] A. S. Markosyan,[51] A. Markowitz,[1] E. Maros,[1] A. Marquina,[104] S. Marsat,[26] F. Martelli,[63,64] I. W. Martin,[46] R. M. Martin,[36] V. Martinez,[79] D. V. Martynov,[13] H. Masalehdan,[134] K. Mason,[14] E. Massera,[112] A. Masserot,[34] T. J. Massinger,[1] M. Masso-Reid,[46] S. Mastrogiovanni,[26] A. Matas,[76] F. Matichard,[1,14] L. Matone,[105] N. Mavalvala,[14] J. J. McCann,[66] R. McCarthy,[47] D. E. McClelland,[8] S. McCormick,[7] L. McCuller,[14] S. C. McGuire,[168] C. McIsaac,[140] J. McIver,[1] D. J. McManus,[8] T. McRae,[8] S. T. McWilliams,[39] D. Meacher,[24] G. D. Meadors,[6] M. Mehmet,[9,10] A. K. Mehta,[18] J. Meidam,[37] E. Mejuto Villa,[116,69] A. Melatos,[100] G. Mendell,[47] R. A. Mercer,[24] L. Mereni,[23] K. Merfeld,[72] E. L. Merilh,[47] M. Merzougui,[65] S. Meshkov,[1] C. Messenger,[46] C. Messick,[90] F. Messina,[44,45] R. Metzdorff,[73] P. M. Meyers,[100] F. Meylahn,[9,10] A. Miani,[117,118] H. Miao,[13] C. Michel,[23] H. Middleton,[100] L. Milano,[80,5] A. L. Miller,[30,119,33] M. Millhouse,[100] J. C. Mills,[106] M. C. Milovich-Goff,[133] O. Minazzoli,[65,169] Y. Minenkov,[32] A. Mishkin,[30] C. Mishra,[170] T. Mistry,[112] S. Mitra,[3] V. P. Mitrofanov,[61] G. Mitselmakher,[30] R. Mittleman,[14] G. Mo,[98] D. Moffa,[121] K. Mogushi,[87] S. R. P. Mohapatra,[14] M. Molina-Ruiz,[141] M. Mondin,[133] M. Montani,[63,64] C. J. Moore,[13] D. Moraru,[47] F. Morawski,[56] G. Moreno,[47] S. Morisaki,[83] B. Mours,[34] C. M. Mow-Lowry,[13] F. Muciaccia,[119,33] Arunava Mukherjee,[9,10] D. Mukherjee,[24] S. Mukherjee,[108] Subroto Mukherjee,[111] N. Mukund,[9,10,3] A. Mullavey,[7] J. Munch,[57] E. A. Muñiz,[42] M. Muratore,[35] P. G. Murray,[46] A. Nagar,[89,127,171] I. Nardecchia,[86,32] L. Naticchioni,[119,33] R. K. Nayak,[172] B. F. Neil,[66] J. Neilson,[116,69] G. Nelemans,[67,37] T. J. N. Nelson,[7] M. Nery,[9,10] A. Neunzert,[137] L. Nevin,[1] K. Y. Ng,[14] S. Ng,[57] C. Nguyen,[26] P. Nguyen,[72] D. Nichols,[142,37] S. A. Nichols,[2] S. Nissanke,[142,37] F. Nocera,[29] C. North,[106] L. K. Nuttall,[140] M. Obergaulinger,[22,173] J. Oberling,[47] B. D. O'Brien,[30] G. Oganesyan,[16,17] G. H. Ogin,[174] J. J. Oh,[152] S. H. Oh,[152] F. Ohme,[9,10] H. Ohta,[83] M. A. Okada,[15] M. Oliver,[101] P. Oppermann,[9,10] Richard J. Oram,[7] B. O'Reilly,[7] R. G. Ormiston,[43] L. F. Ortega,[30] R. O'Shaughnessy,[62] S. Ossokine,[76] D. J. Ottaway,[57] H. Overmier,[7] B. J. Owen,[85] A. E. Pace,[90] G. Pagano,[20,21] M. A. Page,[66] G. Pagliaroli,[16,17] A. Pai,[130] S. A. Pai,[60] J. R. Palamos,[72] O. Palashov,[149] C. Palomba,[33] H. Pan,[91] P. K. Panda,[144] P. T. H. Pang,[94,37] C. Pankow,[58] F. Pannarale,[119,33] B. C. Pant,[60] F. Paoletti,[21] A. Paoli,[29] A. Parida,[3] W. Parker,[7,168] D. Pascucci,[46,37] A. Pasqualetti,[29] R. Passaquieti,[20,21] D. Passuello,[21] M. Patil,[157] B. Patricelli,[20,21] E. Payne,[6] B. L. Pearlstone,[46] T. C. Pechsiri,[30] A. J. Pedersen,[42] M. Pedraza,[1] R. Pedurand,[23,175] A. Pele,[7] S. Penn,[176] A. Perego,[117,118] C. J. Perez,[47] C. Périgois,[34] A. Perreca,[117,118] J. Petermann,[134] H. P. Pfeiffer,[76] M. Phelps,[9,10] K. S. Phukon,[3] O. J. Piccinni,[119,33] M. Pichot,[65] F. Piergiovanni,[63,64] V. Pierro,[116,69] G. Pillant,[29] L. Pinard,[23] I. M. Pinto,[116,69,89] M. Pirello,[47] M. Pitkin,[46] W. Plastino,[164,165] R. Poggiani,[20,21] D. Y. T. Pong,[94] S. Ponrathnam,[3] P. Popolizio,[29] E. K. Porter,[26] J. Powell,[167] A. K. Prajapati,[111] J. Prasad,[3] K. Prasai,[51] R. Prasanna,[144] G. Pratten,[101] T. Prestegard,[24] M. Principe,[116,89,69] G. A. Prodi,[117,118] L. Prokhorov,[13] M. Punturo,[41] P. Puppo,[33] M. Pürrer,[76] H. Qi,[106] V. Quetschke,[108] P. J. Quinonez,[35] F. J. Raab,[47] G. Raaijmakers,[142,37] H. Radkins,[47] N. Radulesco,[65] P. Raffai,[110] S. Raja,[60] C. Rajan,[60] B. Rajbhandari,[85] M. Rakhmanov,[108] K. E. Ramirez,[108] A. Ramos-Buades,[101] Javed Rana,[3] K. Rao,[58] P. Rapagnani,[119,33] V. Raymond,[106] M. Razzano,[20,21] J. Read,[27] T. Regimbau,[34] L. Rei,[59] S. Reid,[25] D. H. Reitze,[1,30] P. Rettegno,[127,177] F. Ricci,[119,33] C. J. Richardson,[35] J. W. Richardson,[1] P. M. Ricker,[19] G. Riemenschneider,[177,127] K. Riles,[137] M. Rizzo,[58] N. A. Robertson,[1,46] F. Robinet,[28] A. Rocchi,[32] L. Rolland,[34] J. G. Rollins,[1] V. J. Roma,[72] M. Romanelli,[71] J. Romano,[85] R. Romano,[4,5] C. L. Romel,[47] J. H. Romie,[7] C. A. Rose,[24] D. Rose,[27] K. Rose,[121] D. Rosińska,[74] S. G. Rosofsky,[19] M. P. Ross,[178] S. Rowan,[46] A. Rüdiger,[9,10,*] P. Ruggi,[29] G. Rutins,[132] K. Ryan,[47] S. Sachdev,[90] T. Sadecki,[47] M. Sakellariadou,[146] O. S. Salafia,[179,44,45] L. Salconi,[29] M. Saleem,[31] A. Samajdar,[37] L. Sammut,[6] E. J. Sanchez,[1] L. E. Sanchez,[1] N. Sanchis-Gual,[180] J. R. Sanders,[181] K. A. Santiago,[36] E. Santos,[65] N. Sarin,[6] B. Sassolas,[23] B. S. Sathyaprakash,[90,106] O. Sauter,[137,34] R. L. Savage,[47] P. Schale,[72] M. Scheel,[48] J. Scheuer,[58] P. Schmidt,[13,67] R. Schnabel,[134] R. M. S. Schofield,[72] A. Schönbeck,[134] E. Schreiber,[9,10] B. W. Schulte,[9,10] B. F. Schutz,[106] J. Scott,[46] S. M. Scott,[8] E. Seidel,[19] D. Sellers,[7] A. S. Sengupta,[182] N. Sennett,[76] D. Sentenac,[29] V. Sequino,[59] A. Sergeev,[149] Y. Setyawati,[9,10] D. A. Shaddock,[8] T. Shaffer,[47] M. S. Shahriar,[58] M. B. Shaner,[133] A. Sharma,[16,17] P. Sharma,[60] P. Shawhan,[77] H. Shen,[19] R. Shink,[183] D. H. Shoemaker,[14] D. M. Shoemaker,[78] K. Shukla,[141] S. ShyamSundar,[60] K. Siellez,[78] M. Sieniawska,[56] D. Sigg,[47] L. P. Singer,[81] D. Singh,[90] N. Singh,[74] A. Singhal,[16,33] A. M. Sintes,[101] S. Sitmukhambetov,[108] V. Skliris,[106] B. J. J. Slagmolen,[8] T. J. Slaven-Blair,[66] J. R. Smith,[27] R. J. E. Smith,[6] S. Somala,[184] E. J. Son,[152] S. Soni,[2] B. Sorazu,[46] F. Sorrentino,[59] T. Souradeep,[3] E. Sowell,[85] A. P. Spencer,[46] M. Spera,[53,54] A. K. Srivastava,[111] V. Srivastava,[42] K. Staats,[58] C. Stachie,[65] M. Standke,[9,10] D. A. Steer,[26] M. Steinke,[9,10] J. Steinlechner,[134,46] S. Steinlechner,[134] D. Steinmeyer,[9,10] S. P. Stevenson,[167] D. Stocks,[51] R. Stone,[108] D. J. Stops,[13] K. A. Strain,[46] G. Stratta,[185,64] S. E. Strigin,[61] A. Strunk,[47] R. Sturani,[186] A. L. Stuver,[187] V. Sudhir,[14] T. Z. Summerscales,[188] L. Sun,[1] S. Sunil,[111] A. Sur,[56] J. Suresh,[83] P. J. Sutton,[106] B. L. Swinkels,[37] M. J. Szczepańczyk,[35] M. Tacca,[37] S. C. Tait,[46] C. Talbot,[6] D. B. Tanner,[30] D. Tao,[1] M. Tápai,[131] A. Tapia,[27] J. D. Tasson,[98] R. Taylor,[1] R. Tenorio,[101] L. Terkowski,[134] M. Thomas,[7] P. Thomas,[47] S. R. Thondapu,[60] K. A. Thorne,[7] E. Thrane,[6] Shubhanshu Tiwari,[117,118] Srishti Tiwari,[135] V. Tiwari,[106] K. Toland,[46] M. Tonelli,[20,21] Z. Tornasi,[46] A. Torres-Forné,[189] C. I. Torrie,[1] D. Töyrä,[13] F. Travasso,[29,41] G. Traylor,[7] M. C. Tringali,[74] A. Tripathee,[137] A. Trovato,[26] L. Trozzo,[190,21] K. W. Tsang,[37] M. Tse,[14] R. Tso,[48] L. Tsukada,[83] D. Tsuna,[83] T. Tsutsui,[83] D. Tuyenbayev,[108] K. Ueno,[83] D. Ugolini,[191] C. S. Unnikrishnan,[135] A. L. Urban,[2] S. A. Usman,[93] H. Vahlbruch,[10] G. Vajente,[1] G. Valdes,[2] M. Valentini,[117,118] N. van Bakel,[37] M. van Beuzekom,[37] J. F. J. van den Brand,[75,37] C. Van Den Broeck,[37,192] D. C. Vander-Hyde,[42] L. van der Schaaf,[37] J. V. VanHeijningen,[66] A. A. van Veggel,[46] M. Vardaro,[53,54] V. Varma,[48] S. Vass,[1] M. Vasúth,[50] A. Vecchio,[13] G. Vedovato,[54] J. Veitch,[46] P. J. Veitch,[57] K. Venkateswara,[178] G. Venugopalan,[1] D. Verkindt,[34] F. Vetrano,[63,64] A. Viceré,[63,64] A. D. Viets,[24] S. Vinciguerra,[13] D. J. Vine,[132] J.-Y. Vinet,[65] S. Vitale,[14] T. Vo,[42] H. Vocca,[40,41] C. Vorvick,[47] S. P. Vyatchanin,[61] A. R. Wade,[1] L. E. Wade,[121] M. Wade,[121] R. Walet,[37] M. Walker,[27] L. Wallace,[1] S. Walsh,[24] H. Wang,[13] J. Z. Wang,[137] S. Wang,[19] W. H. Wang,[108] Y. F. Wang,[94] R. L. Ward,[8] Z. A. Warden,[35] J. Warner,[47] M. Was,[34] J. Watchi,[102] B. Weaver,[47] L.-W. Wei,[9,10]

M. Weinert,[9,10] A. J. Weinstein,[1] R. Weiss,[14] F. Wellmann,[9,10] L. Wen,[66] E. K. Wessel,[19] P. Wessels,[9,10] J. W. Westhouse,[35] K. Wette,[8] J. T. Whelan,[62] B. F. Whiting,[30] C. Whittle,[14] D. M. Wilken,[9,10] D. Williams,[46] A. R. Williamson,[142,37] J. L. Willis,[1] B. Willke,[10,9] W. Winkler,[9,10] C. C. Wipf,[1] H. Wittel,[9,10] G. Woan,[46] J. Woehler,[9,10] J. K. Wofford,[62] J. L. Wright,[46] D. S. Wu,[9,10] D. M. Wysocki,[62] S. Xiao,[1] R. Xu,[109] H. Yamamoto,[1] C. C. Yancey,[77] L. Yang,[120] Y. Yang,[30] Z. Yang,[43] M. J. Yap,[8] M. Yazback,[30] D. W. Yeeles,[106] Hang Yu,[14] Haocun Yu,[14] S. H. R. Yuen,[94] A. K. Zadrożny,[108] A. Zadrożny,[156] M. Zanolin,[35] T. Zelenova,[29] J.-P. Zendri,[54] M. Zevin,[58] J. Zhang,[66] L. Zhang,[1] T. Zhang,[46] C. Zhao,[66] G. Zhao,[102] M. Zhou,[58] Z. Zhou,[58] X. J. Zhu,[6] A. B. Zimmerman,[193] M. E. Zucker,[1,14] and J. Zweizig[1]

The LIGO Scientific Collaboration and the Virgo Collaboration

[1]*LIGO, California Institute of Technology, Pasadena, CA 91125, USA*

[2]*Louisiana State University, Baton Rouge, LA 70803, USA*

[3]*Inter-University Centre for Astronomy and Astrophysics, Pune 411007, India*

[4]*Dipartimento di Farmacia, Università di Salerno, I-84084 Fisciano, Salerno, Italy*

[5]*INFN, Sezione di Napoli, Complesso Universitario di Monte S.Angelo, I-80126 Napoli, Italy*

[6]*OzGrav, School of Physics & Astronomy, Monash University, Clayton 3800, Victoria, Australia*

[7]*LIGO Livingston Observatory, Livingston, LA 70754, USA*

[8]*OzGrav, Australian National University, Canberra, Australian Capital Territory 0200, Australia*

[9]*Max Planck Institute for Gravitational Physics (Albert Einstein Institute), D-30167 Hannover, Germany*

[10]*Leibniz Universität Hannover, D-30167 Hannover, Germany*

[11]*Theoretisch-Physikalisches Institut, Friedrich-Schiller-Universität Jena, D-07743 Jena, Germany*

[12]*University of Cambridge, Cambridge CB2 1TN, United Kingdom*

[13]*University of Birmingham, Birmingham B15 2TT, United Kingdom*

[14]*LIGO, Massachusetts Institute of Technology, Cambridge, MA 02139, USA*

[15]*Instituto Nacional de Pesquisas Espaciais, 12227-010 São José dos Campos, São Paulo, Brazil*

[16]*Gran Sasso Science Institute (GSSI), I-67100 L'Aquila, Italy*

[17]*INFN, Laboratori Nazionali del Gran Sasso, I-67100 Assergi, Italy*

[18]*International Centre for Theoretical Sciences, Tata Institute of Fundamental Research, Bengaluru 560089, India*

[19]*NCSA, University of Illinois at Urbana-Champaign, Urbana, IL 61801, USA*

[20]*Università di Pisa, I-56127 Pisa, Italy*

[21]*INFN, Sezione di Pisa, I-56127 Pisa, Italy*

[22]*Departamento de Astronomía y Astrofísica, Universitat de València, E-46100 Burjassot, València, Spain*

[23]*Laboratoire des Matériaux Avancés (LMA), CNRS/IN2P3, F-69622 Villeurbanne, France*

[24]*University of Wisconsin-Milwaukee, Milwaukee, WI 53201, USA*

[25]*SUPA, University of Strathclyde, Glasgow G1 1XQ, United Kingdom*

[26]*APC, AstroParticule et Cosmologie, Université Paris Diderot, CNRS/IN2P3, CEA/Irfu, Observatoire de Paris, Sorbonne Paris Cité, F-75205 Paris Cedex 13, France*

[27]*California State University Fullerton, Fullerton, CA 92831, USA*

[28]*LAL, Univ. Paris-Sud, CNRS/IN2P3, Université Paris-Saclay, F-91898 Orsay, France*

[29]*European Gravitational Observatory (EGO), I-56021 Cascina, Pisa, Italy*

[30]*University of Florida, Gainesville, FL 32611, USA*

[31]*Chennai Mathematical Institute, Chennai 603103, India*

[32]*INFN, Sezione di Roma Tor Vergata, I-00133 Roma, Italy*

[33]*INFN, Sezione di Roma, I-00185 Roma, Italy*

[34]*Laboratoire d'Annecy de Physique des Particules (LAPP), Univ. Grenoble Alpes, Université Savoie Mont Blanc, CNRS/IN2P3, F-74941 Annecy, France*

[35]*Embry-Riddle Aeronautical University, Prescott, AZ 86301, USA*

[36]*Montclair State University, Montclair, NJ 07043, USA*

[37]*Nikhef, Science Park 105, 1098 XG Amsterdam, The Netherlands*

[38]*Korea Institute of Science and Technology Information, Daejeon 34141, South Korea*

[39]*West Virginia University, Morgantown, WV 26506, USA*

[40]*Università di Perugia, I-06123 Perugia, Italy*

[41]*INFN, Sezione di Perugia, I-06123 Perugia, Italy*

[42]*Syracuse University, Syracuse, NY 13244, USA*

[43]*University of Minnesota, Minneapolis, MN 55455, USA*

[44]*Università degli Studi di Milano-Bicocca, I-20126 Milano, Italy*

[45]*INFN, Sezione di Milano-Bicocca, I-20126 Milano, Italy*

[46]*SUPA, University of Glasgow, Glasgow G12 8QQ, United Kingdom*

[47]*LIGO Hanford Observatory, Richland, WA 99352, USA*

[48]*Caltech CaRT, Pasadena, CA 91125, USA*

[49]*Dipartimento di Medicina, Chirurgia e Odontoiatria "Scuola Medica Salernitana," Università di Salerno, I-84081 Baronissi, Salerno, Italy*

[50]*Wigner RCP, RMKI, H-1121 Budapest, Konkoly Thege Miklós út 29-33, Hungary*
[51]*Stanford University, Stanford, CA 94305, USA*
[52]*Università di Camerino, Dipartimento di Fisica, I-62032 Camerino, Italy*
[53]*Università di Padova, Dipartimento di Fisica e Astronomia, I-35131 Padova, Italy*
[54]*INFN, Sezione di Padova, I-35131 Padova, Italy*
[55]*Montana State University, Bozeman, MT 59717, USA*
[56]*Nicolaus Copernicus Astronomical Center, Polish Academy of Sciences, 00-716, Warsaw, Poland*
[57]*OzGrav, University of Adelaide, Adelaide, South Australia 5005, Australia*
[58]*Center for Interdisciplinary Exploration & Research in Astrophysics (CIERA), Northwestern University, Evanston, IL 60208, USA*
[59]*INFN, Sezione di Genova, I-16146 Genova, Italy*
[60]*RRCAT, Indore, Madhya Pradesh 452013, India*
[61]*Faculty of Physics, Lomonosov Moscow State University, Moscow 119991, Russia*
[62]*Rochester Institute of Technology, Rochester, NY 14623, USA*
[63]*Università degli Studi di Urbino "Carlo Bo," I-61029 Urbino, Italy*
[64]*INFN, Sezione di Firenze, I-50019 Sesto Fiorentino, Firenze, Italy*
[65]*Artemis, Université Côte d'Azur, Observatoire Côte d'Azur, CNRS, CS 34229, F-06304 Nice Cedex 4, France*
[66]*OzGrav, University of Western Australia, Crawley, Western Australia 6009, Australia*
[67]*Department of Astrophysics/IMAPP, Radboud University Nijmegen, P.O. Box 9010, 6500 GL Nijmegen, The Netherlands*
[68]*Dipartimento di Fisica "E.R. Caianiello," Università di Salerno, I-84084 Fisciano, Salerno, Italy*
[69]*INFN, Sezione di Napoli, Gruppo Collegato di Salerno, Complesso Universitario di Monte S. Angelo, I-80126 Napoli, Italy*
[70]*Physik-Institut, University of Zurich, Winterthurerstrasse 190, 8057 Zurich, Switzerland*
[71]*Univ Rennes, CNRS, Institut FOTON - UMR6082, F-3500 Rennes, France*
[72]*University of Oregon, Eugene, OR 97403, USA*
[73]*Laboratoire Kastler Brossel, Sorbonne Université, CNRS, ENS-Université PSL, Collège de France, F-75005 Paris, France*
[74]*Astronomical Observatory Warsaw University, 00-478 Warsaw, Poland*
[75]*VU University Amsterdam, 1081 HV Amsterdam, The Netherlands*
[76]*Max Planck Institute for Gravitational Physics (Albert Einstein Institute), D-14476 Potsdam-Golm, Germany*
[77]*University of Maryland, College Park, MD 20742, USA*
[78]*School of Physics, Georgia Institute of Technology, Atlanta, GA 30332, USA*
[79]*Université de Lyon, Université Claude Bernard Lyon 1, CNRS, Institut Lumière Matière, F-69622 Villeurbanne, France*
[80]*Università di Napoli "Federico II," Complesso Universitario di Monte S.Angelo, I-80126 Napoli, Italy*
[81]*NASA Goddard Space Flight Center, Greenbelt, MD 20771, USA*
[82]*Dipartimento di Fisica, Università degli Studi di Genova, I-16146 Genova, Italy*
[83]*RESCEU, University of Tokyo, Tokyo, 113-0033, Japan.*
[84]*Tsinghua University, Beijing 100084, China*
[85]*Texas Tech University, Lubbock, TX 79409, USA*
[86]*Università di Roma Tor Vergata, I-00133 Roma, Italy*
[87]*The University of Mississippi, University, MS 38677, USA*
[88]*Missouri University of Science and Technology, Rolla, MO 65409, USA*
[89]*Museo Storico della Fisica e Centro Studi e Ricerche "Enrico Fermi," I-00184 Roma, Italy*
[90]*The Pennsylvania State University, University Park, PA 16802, USA*
[91]*National Tsing Hua University, Hsinchu City, 30013 Taiwan, Republic of China*
[92]*Charles Sturt University, Wagga Wagga, New South Wales 2678, Australia*
[93]*University of Chicago, Chicago, IL 60637, USA*
[94]*The Chinese University of Hong Kong, Shatin, NT, Hong Kong*
[95]*Dipartimento di Ingegneria Industriale (DIIN), Università di Salerno, I-84084 Fisciano, Salerno, Italy*
[96]*Seoul National University, Seoul 08826, South Korea*
[97]*Pusan National University, Busan 46241, South Korea*
[98]*Carleton College, Northfield, MN 55057, USA*
[99]*INAF, Osservatorio Astronomico di Padova, I-35122 Padova, Italy*
[100]*OzGrav, University of Melbourne, Parkville, Victoria 3010, Australia*
[101]*Universitat de les Illes Balears, IAC3—IEEC, E-07122 Palma de Mallorca, Spain*
[102]*Université Libre de Bruxelles, Brussels 1050, Belgium*
[103]*Sonoma State University, Rohnert Park, CA 94928, USA*
[104]*Departamento de Matemáticas, Universitat de València, E-46100 Burjassot, València, Spain*
[105]*Columbia University, New York, NY 10027, USA*
[106]*Cardiff University, Cardiff CF24 3AA, United Kingdom*

[107] *University of Rhode Island, Kingston, RI 02881, USA*
[108] *The University of Texas Rio Grande Valley, Brownsville, TX 78520, USA*
[109] *Bellevue College, Bellevue, WA 98007, USA*
[110] *MTA-ELTE Astrophysics Research Group, Institute of Physics, Eötvös University, Budapest 1117, Hungary*
[111] *Institute for Plasma Research, Bhat, Gandhinagar 382428, India*
[112] *The University of Sheffield, Sheffield S10 2TN, United Kingdom*
[113] *IGFAE, Campus Sur, Universidade de Santiago de Compostela, 15782 Spain*
[114] *Dipartimento di Scienze Matematiche, Fisiche e Informatiche, Università di Parma, I-43124 Parma, Italy*
[115] *INFN, Sezione di Milano Bicocca, Gruppo Collegato di Parma, I-43124 Parma, Italy*
[116] *Dipartimento di Ingegneria, Università del Sannio, I-82100 Benevento, Italy*
[117] *Università di Trento, Dipartimento di Fisica, I-38123 Povo, Trento, Italy*
[118] *INFN, Trento Institute for Fundamental Physics and Applications, I-38123 Povo, Trento, Italy*
[119] *Università di Roma "La Sapienza," I-00185 Roma, Italy*
[120] *Colorado State University, Fort Collins, CO 80523, USA*
[121] *Kenyon College, Gambier, OH 43022, USA*
[122] *Christopher Newport University, Newport News, VA 23606, USA*
[123] *CNR-SPIN, c/o Università di Salerno, I-84084 Fisciano, Salerno, Italy*
[124] *Scuola di Ingegneria, Università della Basilicata, I-85100 Potenza, Italy*
[125] *National Astronomical Observatory of Japan, 2-21-1 Osawa, Mitaka, Tokyo 181-8588, Japan*
[126] *Observatori Astronòmic, Universitat de València, E-46980 Paterna, València, Spain*
[127] *INFN Sezione di Torino, I-10125 Torino, Italy*
[128] *School of Mathematics, University of Edinburgh, Edinburgh EH9 3FD, United Kingdom*
[129] *Institute Of Advanced Research, Gandhinagar 382426, India*
[130] *Indian Institute of Technology Bombay, Powai, Mumbai 400 076, India*
[131] *University of Szeged, Dóm tér 9, Szeged 6720, Hungary*
[132] *SUPA, University of the West of Scotland, Paisley PA1 2BE, United Kingdom*
[133] *California State University, Los Angeles, 5151 State University Dr, Los Angeles, CA 90032, USA*
[134] *Universität Hamburg, D-22761 Hamburg, Germany*
[135] *Tata Institute of Fundamental Research, Mumbai 400005, India*
[136] *INAF, Osservatorio Astronomico di Capodimonte, I-80131 Napoli, Italy*
[137] *University of Michigan, Ann Arbor, MI 48109, USA*
[138] *Washington State University, Pullman, WA 99164, USA*
[139] *American University, Washington, D.C. 20016, USA*
[140] *University of Portsmouth, Portsmouth, PO1 3FX, United Kingdom*
[141] *University of California, Berkeley, CA 94720, USA*
[142] *GRAPPA, Anton Pannekoek Institute for Astronomy and Institute for High-Energy Physics, University of Amsterdam, Science Park 904, 1098 XH Amsterdam, The Netherlands*
[143] *Delta Institute for Theoretical Physics, Science Park 904, 1090 GL Amsterdam, The Netherlands*
[144] *Directorate of Construction, Services & Estate Management, Mumbai 400094 India*
[145] *University of Białystok, 15-424 Białystok, Poland*
[146] *King's College London, University of London, London WC2R 2LS, United Kingdom*
[147] *University of Southampton, Southampton SO17 1BJ, United Kingdom*
[148] *University of Washington Bothell, Bothell, WA 98011, USA*
[149] *Institute of Applied Physics, Nizhny Novgorod, 603950, Russia*
[150] *Ewha Womans University, Seoul 03760, South Korea*
[151] *Inje University Gimhae, South Gyeongsang 50834, South Korea*
[152] *National Institute for Mathematical Sciences, Daejeon 34047, South Korea*
[153] *Ulsan National Institute of Science and Technology, Ulsan 44919, South Korea*
[154] *Maastricht University, P.O. Box 616, 6200 MD Maastricht, The Netherlands*
[155] *Bard College, 30 Campus Rd, Annandale-On-Hudson, NY 12504, USA*
[156] *NCBJ, 05-400 Świerk-Otwock, Poland*
[157] *Institute of Mathematics, Polish Academy of Sciences, 00656 Warsaw, Poland*
[158] *Cornell University, Ithaca, NY 14850, USA*
[159] *Hillsdale College, Hillsdale, MI 49242, USA*
[160] *Hanyang University, Seoul 04763, South Korea*
[161] *Korea Astronomy and Space Science Institute, Daejeon 34055, South Korea*
[162] *Institute for High-Energy Physics, University of Amsterdam, Science Park 904, 1098 XH Amsterdam, The Netherlands*

[163] NASA Marshall Space Flight Center, Huntsville, AL 35811, USA
[164] Dipartimento di Matematica e Fisica, Università degli Studi Roma Tre, I-00146 Roma, Italy
[165] INFN, Sezione di Roma Tre, I-00146 Roma, Italy
[166] ESPCI, CNRS, F-75005 Paris, France
[167] OzGrav, Swinburne University of Technology, Hawthorn VIC 3122, Australia
[168] Southern University and A&M College, Baton Rouge, LA 70813, USA
[169] Centre Scientifique de Monaco, 8 quai Antoine Ier, MC-98000, Monaco
[170] Indian Institute of Technology Madras, Chennai 600036, India
[171] Institut des Hautes Etudes Scientifiques, F-91440 Bures-sur-Yvette, France
[172] IISER-Kolkata, Mohanpur, West Bengal 741252, India
[173] Institut für Kernphysik, Theoriezentrum, 64289 Darmstadt, Germany
[174] Whitman College, 345 Boyer Avenue, Walla Walla, WA 99362 USA
[175] Université de Lyon, F-69361 Lyon, France
[176] Hobart and William Smith Colleges, Geneva, NY 14456, USA
[177] Dipartimento di Fisica, Università degli Studi di Torino, I-10125 Torino, Italy
[178] University of Washington, Seattle, WA 98195, USA
[179] INAF, Osservatorio Astronomico di Brera sede di Merate, I-23807 Merate, Lecco, Italy
[180] Centro de Astrofísica e Gravitação (CENTRA), Departamento de Física, Instituto Superior Técnico, Universidade de Lisboa, 1049-001 Lisboa, Portugal
[181] Marquette University, 11420 W. Clybourn St., Milwaukee, WI 53233, USA
[182] Indian Institute of Technology, Gandhinagar Ahmedabad Gujarat 382424, India
[183] Université de Montréal/Polytechnique, Montreal, Quebec H3T 1J4, Canada
[184] Indian Institute of Technology Hyderabad, Sangareddy, Khandi, Telangana 502285, India
[185] INAF, Osservatorio di Astrofisica e Scienza dello Spazio, I-40129 Bologna, Italy
[186] International Institute of Physics, Universidade Federal do Rio Grande do Norte, Natal RN 59078-970, Brazil
[187] Villanova University, 800 Lancaster Ave, Villanova, PA 19085, USA
[188] Andrews University, Berrien Springs, MI 49104, USA
[189] Max Planck Institute for Gravitationalphysik (Albert Einstein Institute), D-14476 Potsdam-Golm, Germany
[190] Università di Siena, I-53100 Siena, Italy
[191] Trinity University, San Antonio, TX 78212, USA
[192] Van Swinderen Institute for Particle Physics and Gravity, University of Groningen, Nijenborgh 4, 9747 AG Groningen, The Netherlands
[193] Department of Physics, University of Texas, Austin, TX 78712, USA

(Dated: August 16, 2019)

ABSTRACT

This paper presents the gravitational-wave measurement of the Hubble constant H_0 using the detections from the first and second observing runs of the Advanced LIGO and Virgo detector network. The presence of the transient electromagnetic counterpart of the binary neutron star GW170817 led to the first standard-siren measurement of H_0. Here we additionally use binary black hole detections in conjunction with galaxy catalogs and report a joint measurement. Our updated measurement is $H_0 = 68^{+14}_{-7}$ km s^{-1} Mpc^{-1} (68.3% highest density posterior interval with a flat-in-log prior) which is a 7% improvement over the GW170817-only value of 68^{+18}_{-8} km s^{-1} Mpc^{-1}. A significant additional contribution currently comes from GW170814, a loud and well-localized detection from a part of the sky thoroughly covered by the Dark Energy Survey. Inclusion of contributions from all binary black hole detections entails a thorough marginalization over unknown population parameters. With numerous detections anticipated over the upcoming years, an exhaustive understanding of other systematic effects are also going to become increasingly important. These results establish the path to cosmology using gravitational-wave observations with and without transient electromagnetic counterparts.

1. INTRODUCTION

Gravitational waves (GWs) from compact binary coalescences allow for a direct measurement of the luminosity distance to their source. This makes them standard-distance indicators, and in conjunction with an identified host galaxy or a set of possible host galaxies, they can be used as "standard sirens" to construct a redshift-distance relationship and measure cosmological parameters like the Hubble constant (H_0) (Schutz 1986; Holz & Hughes 2005; MacLeod & Hogan 2008; Nissanke et al. 2010; Sathyaprakash et al. 2010). The GW signature from the binary neutron star (BNS) merger

* Deceased, July 2018.

GW170817, along with its coincident electromagnetic (EM) transient associated with the host galaxy NGC4993, led to a first standard-siren measurement of H_0 (Abbott et al. 2017b). This measurement is independent of other state-of-the-art measurements of H_0, and in particular, independent of the cosmic distance ladder used to calibrate standardizable sources like Type Ia supernovae. The importance of an independent measurement of H_0 is worth highlighting. With the Planck 2018 data release (Aghanim et al. 2018), and the recent recalibration of supernovae using Large Magellanic Cloud Cepheids (Riess et al. 2019), the tension between early universe measurements of H_0 from Planck and local measurements from the SH0ES project has risen to the 4.4-σ level. Independent measurements using cosmological Baryon Acoustic Oscillations to calibrate Type Ia supernovae via the "inverse distance ladder" (Macaulay et al. 2019) and gravitational lensing of quasars in the nearby universe (H0LiCOW Collaboration, Birrer et al. 2019) favor to some degree the early-universe Planck and the local SH0ES measurements respectively. A complementary measurement of H_0 from the multi-messenger GW astronomy sector[1] would help clarify whether the current tension is a statistical anomaly or evidence for new physics beyond the ΛCDM model of cosmology.

The GW standard-siren measurement in Abbott et al. (2017b) is broadly consistent with other measurements. By combining information from multiple detections, one can improve the accuracy reaching about one percent with $O(100)$ detections in the coming years (Nissanke et al. 2013; Chen et al. 2018; Feeney et al. 2019; Mortlock et al. 2018).

An unambiguous identification of the host galaxy is unlikely for all BNS detections; only a crude estimate of the sky position may be available. Moreover there are sources such as binary black hole (BBH) mergers with no expected EM counterparts. Even in the absence of an EM counterpart, the method outlined in Schutz (1986) can be used: with a set of potential host galaxies identified in a galaxy catalog for each detection, one can build up information by a process of statistical cross-correlation. The method was demonstrated on a set of simulations in Del Pozzo (2012), where a 5% estimate on H_0 was obtained from $O(100)$ detections in an idealized situation of nearby events and complete galaxy catalogs; similar results with projections for third-generation detectors have been obtained in Nair et al. (2018). It has further been shown in Chen et al. (2018) that the main benefit of the galaxy-catalog method would be for the case of multiple well-localized sources.

An understanding of GW selection effects (Abbott et al. 2017b; Chen et al. 2018; Mandel et al. 2019) and features of galaxy catalogs, such as their incompleteness and measurement uncertainties, is necessary for an accurate measurement of H_0. Prescriptions to handle incomplete galaxy catalogs have been outlined in Chen et al. (2018), Fishbach et al. (2019), and Gray et al. (2019), and an extensive study of selection effects including galaxy catalog completeness has been performed in Gray et al. (2019). The simulations in Gray et al. (2019) suggest that possible systematic errors using the current method would be mitigated with catalog completeness fractions of as low as $\sim 25\%$ for $O(100)$ detections. The galaxy-catalog method has been used in Fishbach et al. (2019) to infer H_0 from GW170817 without its optical counterpart. An estimate of H_0 from GW170814 and the photometric redshift catalog from the Dark Energy Survey (DES) Year 3 data has recently been obtained in Soares-Santos et al. (2019).

In this paper we report the first joint GW estimate of H_0 from detections during O1 and O2, the first and second observing runs of the Advanced LIGO and Virgo detector network. For our final result, along with the BNS GW170817, we choose only the BBH detections for which we expect a significant contribution from the galaxies present in the catalog rather than assumptions regarding the population properties of BBHs (see Section 5). These detections are GW150914, GW151226, GW170608, GW170814, and GW170818. While the catalog contribution comes from only the detections for which a significant fraction of potential host galaxies are present in an associated galaxy catalog, we note that even without this catalog contribution there is information available, as all BBH detections contribute via their observed distribution in luminosity distance. This latter contribution is measureable when the underlying astrophysical distribution of sources is known. In an ideal situation, one would jointly estimate the astrophysical population parameters along with H_0. This is not expected to provide significant information at this stage given how uncertain the inferred population parameters are even when H_0 is held fixed (Abbott et al. 2018a). We choose to fix the astrophysical population to a fiducial distribution instead, and perform our analysis with different choices for the mass distribution and binary merger rate with redshift in order to quantify possible systematic effects resulting from this assumption. We set aside a more thorough treatment involving a marginalization over the unknown astrophysical distribution for future work.

The main result of our analysis—a posterior distribution on H_0—is dominated by the contribution from GW170817 with its optical counterpart, with only a modest improvement from the inclusion of the above BBHs. These results, pos-

[1] Cosmological parameters can potentially be inferred from GW observations alone by estimating the redshift using the known physics of neutron stars (Messenger & Read 2012) or their astrophysical mass distribution (Taylor & Gair 2012); however these methods are not expected to find an application in context of the current generation of advanced ground-based detectors.

sibly refined and marginalized over the aforementioned assumptions, can be used as a prior for future GW estimates of H_0. The analysis performed in this paper thus serves as a precursor of future analyses for the third and subsequent observing runs of the Advanced detector network.

The rest of this paper is arranged as follows. We describe our method in Section 2. We summarize the GW detections we use in our analysis and the corresponding EM data in Section 3. Our main results are presented in Section 4, with a more detailed discussion and a study of possible systematic effects in Section 5. We conclude in Section 6 and highlight some future directions and prospects.

Throughout this paper we assume a ΛCDM cosmology and use the best-fit Planck 2015 values of $\Omega_m = 0.308$, $\Omega_\Lambda = 0.692$, respectively for the fractional matter and dark energy densities in the present epoch (Aghanim et al. 2018). Although these parameters enter the redshift-distance relationship central to the method for Bayesian inference of H_0, we have verified that our results are robust with regards to a variation of their values within the current measurement uncertainties.

2. METHOD

We follow and apply the Bayesian analysis described in Gray et al. (2019) to compute the posterior probability density on H_0, given the set $\{D_{\rm GW}\}$ of $N_{\rm det}$ detections and the associated GW data $\{x_{\rm GW}\}$:

$$p(H_0|\{x_{\rm GW}\},\{D_{\rm GW}\}) \propto p(H_0)p(N_{\rm det}|H_0)\prod_i^{N_{\rm det}} p(x_{{\rm GW}i}|D_{{\rm GW}i},H_0)\,. \tag{1}$$

Here, $D_{{\rm GW}i}$ indicates that the event i was detected as a GW, $p(H_0)$ is the prior on H_0, and the term $p(N_{\rm det}|H_0)$ is the likelihood of detecting $N_{\rm det}$ events for the particular value of H_0. The total number of detected events is $N_{\rm det} = R\langle VT\rangle$, where $\langle VT\rangle$ is the surveyed comoving time-volume and $R \equiv \frac{\partial N_s}{\partial V \partial T}$ is the intrinsic astrophysical merger rate in the source frame. If the rate R is marginalized over with a prior $p(R) \propto R^{-1}$, then $p(N_{\rm det}|H_0) = \int p(N_{\rm det}|H_0,R)\,p(R)\,dR$ loses its dependence on H_0 (Fishbach et al. 2018). For simplicity, we make this approximation throughout our analysis. The final term factorises into the individual likelihoods for each detection. In the following, we write out the expressions for a single GW event i, omitting the subscript i for brevity of notation,

$$p(x_{\rm GW}|D_{\rm GW},H_0) = \frac{p(D_{\rm GW}|x_{\rm GW},H_0)p(x_{\rm GW}|H_0)}{p(D_{\rm GW}|H_0)}\,. \tag{2}$$

The denominator, $p(D_{\rm GW}|H_0)$, is evaluated as an integral over all possible $x_{\rm GW}$ (Abbott et al. 2017b; Chen et al. 2018; Mandel et al. 2019):

$$p(D_{\rm GW}|H_0) = \int p(D_{\rm GW}|x_{\rm GW},H_0)\,p(x_{\rm GW}|H_0)\,dx_{\rm GW}\,, \tag{3}$$

where $p(D_{\rm GW}|x_{\rm GW},H_0) = 1$ in the case where the signal-to-noise ratio (SNR) of $x_{\rm GW}$ passes some detection threshold, and 0 in the case where it does not.

2.1. *The electromagnetic counterpart case*

In the presence of an EM counterpart, there is additional information in the EM data which appears as an EM likelihood term; together with this is the assumption, $D_{\rm EM}$, that there has been an EM detection. Thus, for a single event with an EM counterpart,

$$p(x_{\rm GW},x_{\rm EM}|D_{\rm GW},D_{\rm EM},H_0) = \frac{p(x_{\rm GW}|H_0)p(x_{\rm EM}|H_0)}{p(D_{\rm EM}|D_{\rm GW},H_0)p(D_{\rm GW}|H_0)}\,. \tag{4}$$

We assume that the detectability of an EM counterpart is dependent on luminosity distance (as opposed to redshift) because it is flux-limited. As GW detectability is also a function of luminosity distance, we expect $p(D_{\rm EM}|D_{\rm GW},H_0)$ to be a constant that does not depend on H_0. This leads to

$$p(x_{\rm GW},x_{\rm EM}|D_{\rm GW},D_{\rm EM},H_0) \approx \frac{p(x_{\rm GW}|H_0)p(x_{\rm EM}|H_0)}{p(D_{\rm GW}|H_0)}. \tag{5}$$

2.2. *The galaxy-catalog case*

In the absence of an EM counterpart, the analogous data comes from galaxy catalogs which provide a set of galaxies and their associated sky locations, redshifts, and apparent magnitudes. As we are in the regime where the detectability of GW sources extends beyond the distance to which current catalogs are complete, the possibility that the GW host galaxy is not contained in the catalog, because it is too faint, has to be taken into account. This is done by marginalizing over the cases where the host is in the catalog (denoted G), and where it is not (denoted $\bar{G}$):

$$p(x_{\rm GW}|D_{\rm GW},H_0) = \sum_{g=G,\bar{G}} p(x_{\rm GW}|g,D_{\rm GW},H_0)p(g|D_{\rm GW},H_0)\,. \tag{6}$$

We model the galaxy catalog as having an apparent magnitude threshold, $m_{\rm th}$, as galaxy catalogs are flux-limited. This, alongside a set of galaxy parameters, determines the probability that a galaxy is inside or outside the galaxy catalog.

The quantities appearing on the right in Eq. (6) can be written out explicitly as follows. The likelihood when the host galaxy is in the catalog, $p(x_{\rm GW}|G,D_{\rm GW},H_0)$, is converted to a ratio of weighted sums over galaxies present in the catalog:

$$p(x_{\rm GW}|G,D_{\rm GW},H_0) = \frac{\sum_{j=1}^{N_{\rm gal}}\int p(x_{\rm GW}|z_j,\Omega_j,H_0)p(s|M(z_j,m_j,H_0))p(z_j)dz_j}{\sum_{j=1}^{N_{\rm gal}}\int p(D_{\rm GW}|z_j,\Omega_j,H_0)p(s|M(z_j,m_j,H_0))p(z_j)dz_j}\,. \tag{7}$$

Here, $N_{\rm gal}$ is the total number of galaxies in the galaxy catalog. Ω_j, and m_j are respectively the sky coordinates and apparent magnitude for galaxy j, and $p(z_j)$ is a Gaussian distribution representing the redshift of galaxy j, using the mean and standard deviation of z provided in the galaxy catalog (see section 3.4.1 for details). $M(z_j, m_j, H_0)$ is the absolute magnitude (for the given H_0), and $p(s|M(z_j, m_j, H_0))$ is the probability of a galaxy with these parameters to host a GW source during the observation time, relative to other galaxies. Formally, s is the statement that a GW has been *sourced* or *emitted* (as opposed to being *detected*); the previous expressions are all implicitly conditioned on the assumption of s. In writing $p(s|M)$, we make the approximation that the probability of a galaxy hosting a source depends only on the intrinsic luminosity of the galaxy, and not on its other parameters or on the properties of the GW source. In essence, this term allows for weighting galaxies by their luminosities $L(M_j(H_0))$ as

$$p(s|M(z_j, m_j, H_0)) \propto \begin{cases} \text{constant}, & \text{if unweighted.} \\ L(M_j(H_0)), & \text{if luminosity-weighted.} \end{cases} \tag{8}$$

The likelihood when the host galaxy is not in the catalog, $p(x_{\rm GW}|\bar{G}, D_{\rm GW}, H_0)$, is a ratio of marginalized integrals:

$$p(x_{\rm GW}|\bar{G}, D_{\rm GW}, H_0) = \frac{\iiint_{z(m_{\rm th},M,H_0)}^{\infty} p(x_{\rm GW}|z,\Omega,H_0)p(z)p(\Omega)p(M|H_0)p(s|M)dzd\Omega dM}{\iiint_{z(m_{\rm th},M,H_0)}^{\infty} p(D_{\rm GW}|z,\Omega,H_0)p(z)p(\Omega)p(M|H_0)p(s|M)dzd\Omega dM}\,. \tag{9}$$

Here the fact that the terms are conditioned on $\bar{G}$ is incorporated into the redshift limits as a function of the apparent magnitude threshold $m_{\rm th}$ of the galaxy catalog. Finally, the prior probabilities that a given GW detection has or does not have support in the galaxy catalog are respectively

$$p(G|D_{\rm GW}, H_0) = \frac{\iiint_{0}^{z(m_{\rm th},M,H_0)} p(D_{\rm GW}|z,\Omega,H_0)p(z)p(\Omega)p(M|H_0)p(s|M)dzd\Omega dM}{\iiint_{0}^{\infty} p(D_{\rm GW}|z,\Omega,H_0)p(z)p(\Omega)p(M|H_0)p(s|M)dzd\Omega dM}, \quad \text{and } p(\bar{G}|D_{\rm GW}, H_0) = 1 - p(G|D_{\rm GW}, H_0). \tag{10}$$

In Eq. (9) and (10), $p(z)$ is the prior on the redshift of host galaxies of GW events, taken to be of the form

$$p(z) \propto \frac{1}{1+z}\frac{dV_{\rm c}(z)}{dz}R(z)\,. \tag{11}$$

Here $V_{\rm c}(z)$ is the comoving volume as a function of redshift and the factor $(1+z)^{-1}$ converts the merger rate from source-frame to detector-frame. The merger rate density may in general be a function of redshift; however we set $R(z) =$ constant throughout (other than in Section 5, where we consider an alternative redshift-dependent rate model). The prior on the GW sky location $p(\Omega)$ is taken to be uniform across the sky. The term $p(M|H_0)$ is the prior on absolute magnitudes for all the galaxies in the universe (not just those inside the galaxy catalog), which we set to follow the Schechter luminosity function:

$$p(M|H_0) \propto 10^{-0.4(\alpha+1)(M-M^*(H_0))}\exp(-10^{-0.4(M-M^*(H_0))}). \tag{12}$$

Following Gehrels et al. (2016), we use B-band luminosity function parameters $\alpha = -1.07$ for the slope of the Schechter function and $M^*(H_0) = -20.47 + 5\log_{10} h$ for its characteristic absolute magnitude[2] (with $h \equiv H_0/100\,{\rm km\ s^{-1}\ Mpc^{-1}}$), throughout the paper. For the upper limits of integration over M, we choose the magnitude of the dimmest galaxies to be $-12.96 + 5\log_{10} h$. The integrals are not sensitive to the choice of their lower limits, *i.e.* the magnitudes of the brightest galaxies. We note that more complex models for $p(M|H_0)$ can be used, in fact, we expect the luminosity distribution of galaxies to also evolve with redshift (Caditz & Petrosian 1989), as well as to depend on galaxy type and color (Madgwick et al. 2002). While the consideration of such dependence is beyond the scope of the current work, we refer the reader to Gray et al. (2019) for a brief discussion on the misspecification of the luminosity function parameters.

Further details and complete derivations for the framework described above are discussed in Gray et al. (2019).

[2] The absolute magnitude is related to the intrinsic luminosity of a galaxy by the relation, $M - M^* \equiv -2.5\log_{10}(L/L^*)$. The parameter M^* of the Schechter function itself depends on H_0, which we take into account.

3. DATA

3.1. *Gravitational-wave data*

The GW searches performed during the first and the second observation runs of Advanced LIGO and Virgo have led to the identification of ten BBH and one BNS mergers (Abbott et al. 2018b). The BNS event GW170817, well-localized and at a nearby distance of 40^{+10}_{-10} Mpc, helped discover the electromagnetic transient from the merger, and was subsequently associated with host galaxy NGC4993. The BBHs span a large range of distances from 320^{+120}_{-110} to 2840^{+1400}_{-1360} Mpc and are distributed over the sky with 90% credible re-

gions as low as 39 deg^2 to as high as 1666 deg^2. A summary of the relevant parameters of all the GW detections are given in Table 1.

3.2. *Galaxy Catalogs*

The analysis with BBHs is performed in conjunction with appropriate galaxy catalogs. For each detection, we attempt to choose the (publicly available) galaxy catalog which is the most complete within the sky localization region and redshift range of a given event (and within our prior bounds on H_0). We use the GLADE catalog (Dálya et al. 2018) as a default, due to its depth and coverage over an extensive region of the sky (see Section 3.2.1). For the GW observations that are particularly well-localized, namely GW170814 and GW170818, certain galaxy catalogs show a clear improvement in completeness over GLADE within the relevant localization volume of the event. In particular, we use the DES Year 1 (Y1A1 GOLD or simply Y1) catalog (Drlica-Wagner et al. 2018; Abbott et al. 2018d) (see Section 3.2.2) for the analysis of GW170814 and the GWENS catalog (Rahman et al. 2019) (based on the SDSS DR14 survey) (see Section 3.2.3) for the analysis of GW170818.

In Table 1 we summarize the galaxy catalogs that we use for our analysis for each of the detections, along with the number of galaxies in the 90% error volume calculated from 3D skymaps constructed from posterior samples associated with the data release of Abbott et al. (2018b)[3], and the estimated completeness in the 90% error region by assuming a Planck 2015 cosmology.

In the following, we describe in more detail the galaxy catalogs that we use, quantify the probability that the host galaxy for each event is in the galaxy catalog that is used for its analysis and discuss the assessment of the completeness over the relevant localization volume for the best localized events. We also discuss how we obtain the B-band luminosities (used for luminosity weighting) by performing photometric transformations from magnitudes in other bands when B-band magnitudes are not available in catalogs. Finally, we quantify the uncertainties associated with the photometric measurement of redshifts in some of these catalogs.

3.2.1. *GLADE*

We use the Galaxy List for the Advanced Detector Era (GLADE) version 2.3 galaxy catalog[4] (Dálya et al. 2018) to construct the observed redshift distributions for the majority of the detected BBHs. The GLADE catalog has an all sky coverage (Fig. 1 of Dálya et al. 2018) since it is constructed from the GWGC, 2MPZ, 2MASS XSC, HyperLEDA and SDSS-DR12Q catalogs. The GLADE catalog is complete (in B-band luminosity) out to 37 Mpc and has an estimated completeness of 50% out to 91 Mpc (Fig. 2 of Dálya et al. 2018). At low redshifts ($\lesssim$ 0.05), we expect to be dominated by the peculiar velocity field. GLADE reports peculiar-velocity-corrected redshifts (in the heliocentric frame) following the reconstruction of Carrick et al. (2015). We also correct all heliocentric redshifts to the cosmic microwave background reference frame (Hinshaw et al. 2009). GLADE provides apparent magnitudes in the B-band, which we can use directly (*i.e.* without any photometric transformations) for luminosity weighting of the galaxies.

3.2.2. *DES Year 1*

The Dark Energy Survey (DES) is an on-going, five year survey that, when completed, will map $\approx$ 300 million galaxies in five filters (*grizY*) over 5000 deg^2. It is worth noting that the GW170814 sky localization is fully enclosed within the footprint of the DES (Drlica-Wagner et al. 2018; Abbott et al. 2018d) Year 3 (Y3) "gold" catalog. An estimate of H_0 from the GW170814 distance and the Y3 catalog of the DES has been carried out (Soares-Santos et al. 2019). In this work, we use the publicly available DES-Y1 catalog[5] (Abbott et al. 2018d) to compute the H_0 posterior for GW170814. We note that $\approx$ 87% of the 99% probability region for the GW170814 sky localization is enclosed within the DES-Y1 catalog. Analysis with a different catalog provides a parallel measurement of H_0 with GW170814, and (given the catalog differences) can potentially be indicative of systematic effects in the catalogs, such as the treatment of redshift uncertainties (provided that a similar set of galaxies are present in both catalogs, including the true host).

The photometric redshifts in the DES-Y1 catalog are estimated using the `ANNz2` (Sadeh et al. 2016) machine learning based photometric redshift algorithm — we defer a brief discussion of some of the potential systematic effects of using specific algorithms to Section 3.4. We use the median photometric redshifts provided in the catalog and discard (around 10%) galaxies with redshift errors larger than their corresponding quoted median redshift value. Such a choice is not expected to strongly bias our result since the discarded galaxies are accounted for by the out-of-catalog term.

In order to obtain B-band magnitudes for the DES survey, we first convert from the DES *grizY* magnitudes to the SDSS *ugriz* system using the photometric transformations provided in the DES-Y1 paper (Drlica-Wagner et al. 2018). We then apply the photometric transformations for galaxies in SDSS given in Cook et al. (2014), where we use the *r* and *i* magnitudes to obtain B-band magnitudes, to be used for luminosity weighting. Finally, we correct all redshifts from the heliocentric to CMB reference frame (Hinshaw et al. 2009).

[3] Available at: https://www.gw-openscience.org/GWTC-1

[4] GLADE is publicly available at: http://glade.elte.hu

[5] DES-Y1 is available at: https://des.ncsa.illinois.edu/releases/y1a1

Event	$\Delta\Omega/\mathrm{deg}^2$	d_L/Mpc	z_{event}	V/Mpc^3	Galaxy catalog	Number of galaxies	$p(G\|z_{\mathrm{event}}, D_{\mathrm{GW}})$
GW150914	182	440^{+150}_{-170}	$0.09^{+0.03}_{-0.03}$	3.5×10^6	GLADE	4944	0.61
GW151012	1523	1080^{+550}_{-490}	$0.21^{+0.09}_{-0.09}$	5.8×10^8	GLADE	45214	0.06
GW151226	1033	450^{+180}_{-190}	$0.09^{+0.04}_{-0.04}$	2.4×10^7	GLADE	39387	0.60
GW170104	921	990^{+440}_{-430}	$0.20^{+0.08}_{-0.08}$	2.4×10^8	GLADE	48786	0.10
GW170608	392	320^{+120}_{-110}	$0.07^{+0.02}_{-0.02}$	3.4×10^6	GLADE	20883	0.76
GW170729	1041	2840^{+1400}_{-1360}	$0.49^{+0.19}_{-0.21}$	8.7×10^9	GLADE	34100	< 0.01
GW170809	308	1030^{+320}_{-390}	$0.20^{+0.05}_{-0.07}$	9.1×10^7	GLADE	23031	0.08
GW170814	87	600^{+150}_{-220}	$0.12^{+0.03}_{-0.04}$	4.0×10^6	DES-Y1	4392112	> 0.99
GW170817	16	40^{+7}_{-15}	$0.01^{+0.00}_{-0.00}$	227	–	–	–
GW170818	39	1060^{+420}_{-380}	$0.21^{+0.07}_{-0.07}$	1.5×10^7	GWENS	134040	0.94
GW170823	1666	1940^{+970}_{-900}	$0.35^{+0.15}_{-0.15}$	3.5×10^9	GLADE	54786	< 0.01

Table 1. Relevant parameters of the O1 and O2 detections: 90% sky localization region $\Delta\Omega$ (deg^2), luminosity distance d_L (Mpc, median with 90% credible intervals), and estimated redshift z_{event} (median with 90% range assuming Planck 2015 cosmology) from Abbott et al. (2018b). In the remaining columns we report the corresponding 90% 3D localization comoving volumes, and the number of galaxies within each volume for public catalogs which we find to be the most complete. The final column gives the probability that the host galaxy is inside the galaxy catalog for each event, $p(G|z_{\mathrm{event}}, D_{\mathrm{GW}})$, also evaluated at the median redshift for each event.

3.2.3. *GWENS*

The Gravitational Wave Events in Sloan (GWENS) galaxy catalog[6] (Rahman et al. 2019) is a curated catalog based on the Data Release 14 (DR14) of the Sloan Digital Sky Survey (SDSS). We use the GWENS catalog to compute the posterior probability on H_0 for GW170818; it is the best sky-localized BBH to date as shown in Table 1 and entirely within the footprint of the SDSS survey. It is worth noting that although the 90% sky localization region is 39 deg^2, the estimated luminosity distance has support out to a distance of around 1450 Mpc, which corresponds to a redshift of 0.28 (assuming a Planck 2015 cosmology); so the completeness of GLADE for this event is insufficient for its analysis.

The GWENS catalog provides photometric redshifts for all galaxies as well as spectroscopic redshift information for a sub-sample of its galaxies where available. The photometric redshift algorithm is based on a hybrid technique: local regression on a spectroscopic training set followed by spectroscopic template fitting (Beck et al. 2016). The GWENS catalog excludes galaxies that have redshift estimates $\sigma_z/z > 0.2$ at the 2-σ level or greater and has a quoted photometric completeness of more than 95% for r-band magnitudes ($r < 21.8$) (Rahman et al. 2019). The completeness fraction was established through comparisons with deeper photometric fields such as COMBO survey (Wolf et al. 2001). GWENS provides apparent magnitude information in the SDSS *ugriz* filter system. In order to obtain B-band magnitudes for GWENS, we apply the photometric transformations for galaxies in SDSS given in Cook et al. (2014) as explained in Section 3.2.2. Finally, we also correct all redshifts from the heliocentric to CMB reference frame (Hinshaw et al. 2009).

[6] GWENS is available at: https://astro.ru.nl/catalogs/sdss_gwgalcat

3.3. *Probability that the host galaxy is in the catalog*

In this work, we assume that we can characterize the completeness of a galaxy catlog using an apparent magnitude threshold (limiting magnitude) m_{th}. We estimate m_{th} by calculating the median value from the apparent magnitude distribution of all the galaxies within the respective catalog. Our estimate is robust when compared to quoted magnitude limits for each catalog from the literature. Moreover our final results are insensitive to differences of $O(1)$ in the choice of m_{th}. The estimated m_{th} thus acts as a suitable tracer, which we use as the average m_{th} for the catalog over the entire sky. Galaxy catalogs are directional, and a more sophisticated analysis would involve calculating the limiting magnitude for a given line of sight. Obtaining the H_0 posterior distribution would thus require a joint estimate of m_{th} along the lines of sights within an event's sky localization. We leave this for future work. That the completeness of a galaxy catalog is modelled by a set of limiting magnitude thresholds, can by itself be a non-trivial assumption, especially for photometric catalogs, since galaxies may be missing for various reasons

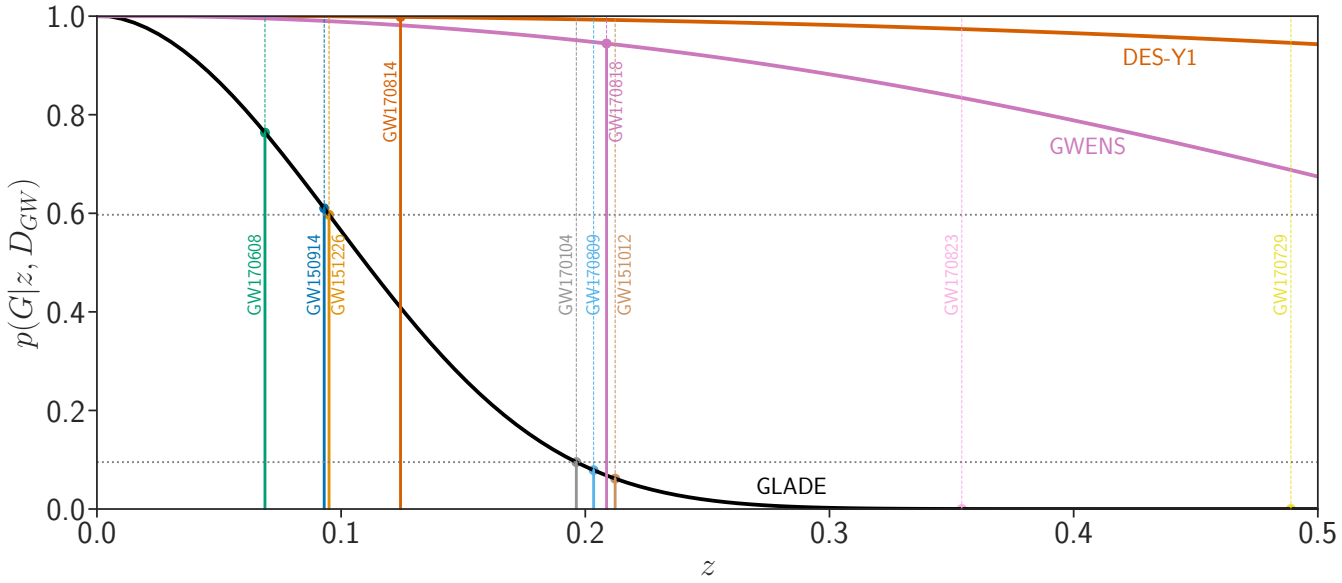

Figure 1. The probability that the host galaxy is inside the galaxy catalog, shown for GLADE (black curve), DES-Y1 (orange curve) and GWENS (pink curve), as a function of redshift. For GLADE this quantity is calculated as an average across the whole sky. For DES-Y1 and GWENS, these curves are only valid in the patches of sky covering GW170814 and GW170818 respectively. Each curve is independent of the value of H_0. The vertical lines show the median redshift (assuming a Planck 2015 cosmology) for each event as in Table 1. These lines are thick and solid up to the intercept with the galaxy catalog they are used with, and thin and dashed above. Also shown is the gap between the lowest value for $p(G|z, D_{\rm GW})$ for the events which are used in the final analysis, and the highest value of $p(G|z, D_{\rm GW})$ for the events which are excluded from the analysis (horizontal dotted grey lines).

other than them being too faint. This will also need to be revisited in the future in a catalog-specific manner.

For now, we use the $m_{\rm th}$ estimated as described above, and show in Fig.1 the probability of a host galaxy being inside the catalog $p(G|z, D_{\rm GW})$ as a function of redshift z, for each of the galaxy catalogs under consideration. For GLADE this quantity is calculated as an average across the whole sky. For DES-Y1 and GWENS, these curves are for the patches of sky covering GW170814 and GW170818 respectively. These probability distributions are calculated using the expressions in Eq. (10), but only over a range of z values and not integrating over z. These expressions by themselves are independent of the choice of H_0. We additionally show as the vertical lines in Fig. 1 the median redshift for each event $z_{\rm event}$ (calculated assuming a Planck 2015 cosmology).

In Fig. 1, we see that the BBHs fall into two categories: those for which there is a high probability that the host galaxy is in one of the catalogs, $p(G|z_{\rm event}, D_{\rm GW}) > 60\%$ (henceforth "high in-catalog probability"), and those for which this probability is very low, $p(G|z_{\rm event}, D_{\rm GW}) < 20\%$ (henceforth "low in-catalog probability"). In order to reduce the effects of systematics which are dominant in events with very little support in the catalog (see Section 5 for details), we choose to include only BBHs from the former "high in-catalog probability" group in our final analysis. This group consists of GW150914, GW151216 and GW170608 with the GLADE catalog, GW170814 with the DES-Y1 catalog, and GW170818 with the GWENS catalog. This choice ensures that the BBH contribution in our final result is driven by the information in the galaxy catalogs, rather than by prior assumptions.

3.4. *Detailed analysis of DES-Y1 and GWENS*

Since the GW170814 and GW170818 events are the best localized BBH events to date, we analyze these with the DES-Y1 and GWENS galaxy catalogs respectively. Both of these catalogs are expected to be more complete than GLADE since these have limiting magnitudes of approximately 23.5 for DES-Y1 and 22 for GWENS in r-band, whereas GLADE has a limiting magnitude of approximately 19.5 in B-band. The higher completeness fraction of DES-Y1 and GWENS within the GW170814 and GW170818 is apparent from Fig. 1. It is helpful to have a detailed assessment of the contribution from potential host galaxies as a function of redshift for these events. We perform a treatment analogous to Fishbach et al. (2019) and compute the ratio $p_{\rm cat}(z)/p_{\rm vol}(z)$ between the probability distribution for the redshifts of potential host galaxies $p_{\rm cat}(z)$ and of a uniform in comoving volume distribution of galaxies $p_{\rm vol}(z)$. When computing $p_{\rm cat}(z)$ we include all galaxies brighter than $0.001L^*_B$ within the corresponding event's 99% sky localization region defined as,

$$p_{\rm cat}(z) \equiv \int p(x_{\rm GW}|\Omega)\, p_0(z, \Omega)\, d\Omega\,, \qquad (13)$$

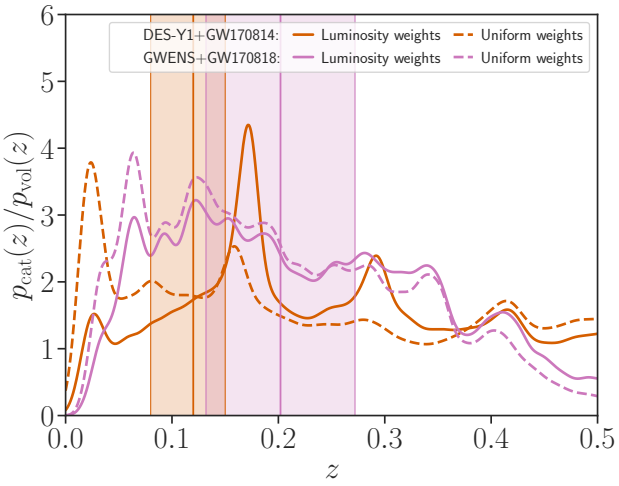

Figure 2. Probability distributions for the redshifts of potential host galaxies $p_{\rm cat}(z)$ divided out by a uniform in comoving volume distribution $p_{\rm vol}(z)$ of galaxies. When computing $p_{\rm cat}(z)$ we include all galaxies brighter than $0.005L_B^*$ within the corresponding event's 99% sky localization region and weight each galaxy by weights proportional to their B-band luminosity (solid lines) as well as with uniform weights (dashed lines). We show these distributions for the DES-Y1 galaxies within the GW170814 sky localization region (orange) and for the GWENS galaxies within the GW170818 sky localization region (pink). These curves trace the over/under density of galaxies, and then fall off at larger redshift due to incompleteness in the catalog. We also show the 90% median estimated redshift ranges for both GW170814 and GW170818 (calculated assuming a Planck 2015 cosmology) for reference.

where $p(x_{\rm GW}|\Omega)$ is the GW likelihood as a function of the sky position Ω (this effectively weights each galaxy with the 2D skymap probability), and $p_0(z,\Omega)$ represents the galaxy catalog contribution, obtained from the distribution of galaxies in the catalog weighted by their probability of hosting a GW source (assuming a Planck 2015 cosmology for the required magnitude conversion). We consider weights for each galaxy proportional to their B-band luminosity as well as uniform weights to explore the effects due to this choice. In order to prevent artificial clustering in $p_{\rm cat}(z)$, we use a Monte Carlo draw for the redshift as opposed to the median value (as explained in Section 3.4.1).

In Fig. 2 we show the distributions $p_{\rm cat}(z)/p_{\rm vol}(z)$ for the DES-Y1 and GWENS galaxies within the GW170814 and GW170818 sky localization regions respectively, for the redshift range $0 < z < 0.5$. These curves trace the over/under density of galaxies, and then fall off at larger redshift due to incompleteness in the catalog. There are regions with higher density in the number of galaxies at redshifts of around 0.02, 0.17 and 0.29 for DES-Y1, and around 0.07 and 0.12 for GWENS for both luminosity and uniform weights cases. We note that these features are more pronounced for the luminosity weighted case at large redshifts. This is expected, as the luminosity weights give higher probability to the luminous galaxies which serve as tracers for the matter distribution of galaxies (these are biased tracers of the underlying clustered matter distribution). The host galaxies for GW170814 and GW170818 are more likely to be located near these higher galaxy density regions in the DES-Y1 and GWENS catalogs – these features in the redshift prior are expected to drive the inferred H_0 posteriors for the corresponding events. We would like to point out that the features we see in the DES-Y1 catalog are not as pronounced as the overdensity in the DES-Y3 data seen in Soares-Santos et al. (2019). This difference is likely driven by the difference in the photometric redshift estimation algorithms, namely, `ANNz2` (Sadeh et al. 2016) and the Directional Neighbourhood Fitting (DNF) method (De Vicente et al. 2016), used respectively in preparation of the DES-Y1 and Y3 catalogs. The different selection criteria for choosing galaxies from the two catalogs, such as the stringent redshift cut placed in Soares-Santos et al. (2019) versus a more relaxed redshift prior used in this work, is another potential source of difference between the corresponding redshift distributions.

3.4.1. *Redshift uncertainties*

An important source of measurement uncertainty with galaxy catalogs is the photometric estimation of redshifts due to a lack of spectroscopic measurements out to large redshifts. In order to account for systematic effects arising from the photometric estimation of redshifts, we perform a marginalization over the redshift uncertainty. For the estimated redshift of each galaxy, we model a Gaussian distribution with a mean of $z_{\rm photo}$ and standard deviation of $\sigma_{z_{\rm photo}}$ (for the DES-Y1 catalog, this is estimated from the random Monte Carlo draw provided for each of the galaxies in the catalog), and marginalize over this uncertainty by randomly sampling $N_{\rm photo} = 100$ times from this distribution, to wash out any structure introduced by the photometric algorithms. The integral over z_j in Eq. (7) becomes an additional sum over $N_{\rm photo}$ samples. We verify that $N_{\rm photo} \sim O(100)$ galaxies is large enough to not introduce any significant errors due to the random sampling.

4. RESULTS

We apply the method described above to obtain a measurement of the Hubble constant using GW standard sirens only. We carry out our analysis with a prior on H_0 uniform in the interval of [20, 140] km s^{-1} Mpc^{-1}; we report our final results also using a flat-in-log prior $p(H_0) \propto H_0^{-1}$ in the same interval for ease of comparison with previous studies. We use the marginalized distance likelihood and skymaps con-

structed from the posterior samples of Abbott et al. (2018b)[7]. For the BBHs, we choose all galaxies in the 99.9% sky region of the corresponding catalog and redshift ranges that allow for the full support of the distance distribution given the H_0 prior. We further weight the galaxies in proportion to the Schechter distribution of their B-band luminosities. In order to calculate the term $p(D_{\rm GW}|H_0)$ in the denominator, we use a Monte Carlo integration, sampling parameters which affect an event's detectability (masses, sky location, inclination angle, and polarisation) from chosen priors. We choose a power-law mass distribution for BBHs with $p(m_1) \propto m_1^{-\alpha}$ and m_2 uniform in its range with $5M_\odot < m_2 < m_1 < 40M_\odot$ in the source frame, and a distribution of merger rates that does not evolve with redshift; for the power-law index α, we choose $\alpha = 1.6$ (which is supported by Model B of Abbott et al. 2018a). For BNSs, we use a Gaussian mass distribution with a mean of $1.35M_\odot$ and a standard deviation of $0.15M_\odot$ (Kiziltan et al. 2010). The remaining GW parameters are marginalized over their natural distributions: uniform in the sky, uniform on the sphere for orientation, uniform in polarization. We use the time-averaged power-spectral-density of detector noise for the corresponding observation run from Abbott et al. (2018c), and for the detection criterion, we use an SNR threshold of $\rho_{\rm th} = 8$ for at least two of the detectors in the detector network. We note that in practice a detection is claimed not solely on the basis of the SNR, but additionally by applying data quality vetoes in order to remove noise transients, and eventually constructing a ranking statistic such as an inverse false alarm rate or a likelihood-ratio (Abbott et al. 2018b). While a careful treatment should use a threshold on a ranking statistic rather than the SNR as the detection criterion, a distinction between the two does not cause an appreciable difference when only a handful of detections significantly louder than transient noise artifacts are considered (see, *e.g.* , Appendix A.1 of Abbott et al. 2018a).

Our result for the O1 and O2 BBH detections is shown in Fig. 3. The detections for which there is considerable support from the galaxies present in the catalog show features of the galaxy catalog in their H_0 posterior distribution. The GW170814 estimate is qualitatively similar to the result in Soares-Santos et al. (2019) with analogous peaks in the posterior distribution. The differences in peak locations and widths between the two are consistent with the large statistical uncertainties in the measurement and can be attributed to a difference in the redshift distribution for the DES-Y3 catalog used in Soares-Santos et al. (2019) versus that for the public DES-Y1 catalog used in this work. For the detections for which the galaxy catalogs are relatively empty, we see the features of the assumptions on mass distribution and redshift evolution of binary merger rate that have entered our analysis. The more distant events such as GW170729 lead to H_0 estimates pushed to the lower end of the prior.

A thorough treatment in absence of a known BBH population would involve a marginalization over all possible mass distributions and rate models. For our current final result, we choose only the BBH detections with a "high in-catalog probability" for which there is a significant contribution from the galaxies present in the catalog. These events are GW150914, GW151226, GW170608, GW170814, and GW170818. The following section demonstrates that the assumptions on the population distribution make a less severe difference for this choice of detections, and in particular, systematic effects are smaller than statistical uncertainties.

For our final result we combine the contribution of the BBHs above with the result from GW170817 obtained using the low spin prior samples from Abbott et al. (2018b) and an estimated Hubble velocity of $v_H \equiv cz = 3017 \pm 166 \mathrm{kms}^{-1}$ (where c is the speed of light) for NGC4993 from Abbott et al. (2017b). Our final combined result is shown in Fig. 4, with the posterior distribution plotted assuming a uniform H_0 prior: we obtain $H_0 = 68^{+16}_{-8}\,\mathrm{km\,s^{-1}\,Mpc^{-1}}$ (68.3% highest density posterior interval). To compare with values in the literature, we also use a flat-in-log prior, $p(H_0) \propto H_0^{-1}$, and calculate $H_0 = 68^{+14}_{-7}\ \mathrm{km\,s^{-1}\,Mpc^{-1}}$, which corresponds to a 7% improvement over the GW170817-only value of 68^{+18}_{-8} $\mathrm{km\,s^{-1}\,Mpc^{-1}}$.

5. ANALYSIS OF SYSTEMATIC EFFECTS

In this section, we repeat the analysis with alternative population models and assumptions, finding no significant differences with the results presented in Section 4 above, and discuss other possible sources of systematic effects.

5.1. *Population model*

We first test the sensitivity to our assumptions regarding the population model, *i.e.* the mass distribution and the distribution of binary merger rate with redshift. In addition to the power-law mass distribution with $\alpha = 1.6$ (median inferred value using Model B of Abbott et al. 2018a), we choose a shallower flat-in-log mass distribution with $\alpha = 1$, and a steeper distribution with $\alpha = 2.3$ (also within the support of the inferred range). We also relax our assumption on the evolution of rate of binary mergers with redshift. A constant merger rate density, $R(z) =$ constant, implicit in the previous treatment, assumed that the merger rate traces the comoving volume. In addition, we repeat our analysis using a merger rate $R(z) \propto (1+z)^3$, which traces the star formation rate at low redshifts ($z < 2.5$) (Saunders et al. 1990). These relaxed assumptions thus cover a large fraction of physically viable

[7] The posterior parameter distribution has been sampled with a prior $\propto d_L^2$; we remove the effect of this prior a posteriori. For computational convenience, we separately construct a marginalized distance likelihood and a two-dimensional skymap; this approximation will be revisited in the future.

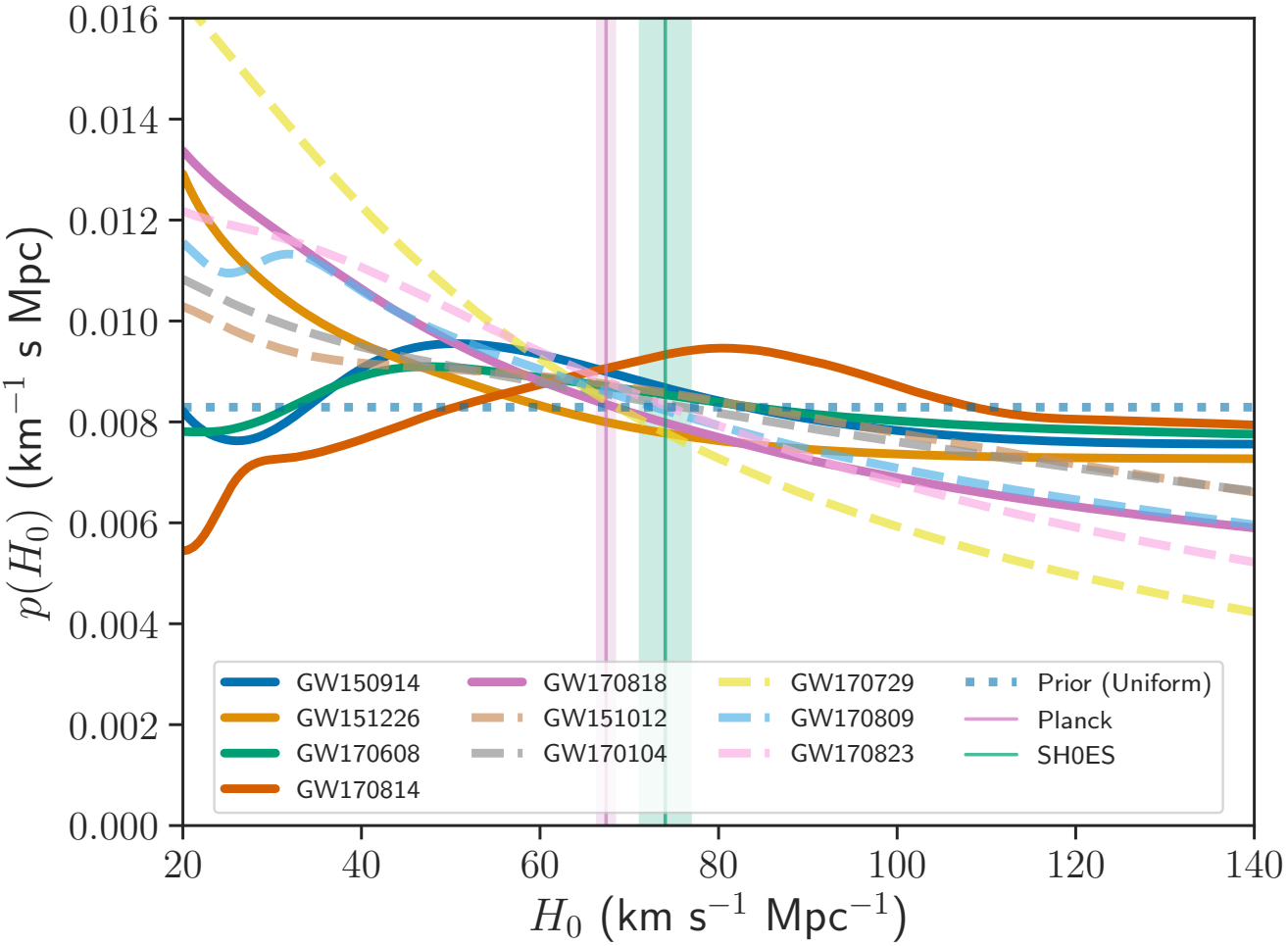

Figure 3. Individual estimates of H_0 from the ten binary black hole detections. These results assume a $m^{-1.6}$ power-law distribution on masses and a non-evolving rate model. Estimates from the "high in-catalog probability" detections with $p(G|z_{\rm event}, D_{\rm GW}) > 60\%$ are shown as solid lines – these are the contributions that go into our final result. Estimates from the remaining detections unused in our final result are shown as dashed lines. All results assume a prior on H_0 uniform in the interval $[20, 140]$ km s^{-1} Mpc^{-1}(dotted blue). We also show the estimates of H_0 from CMB (Planck: Aghanim et al. 2018) and supernova experiments (SH0ES: Riess et al. 2016).

and inferred population models (Abbott et al. 2018a). We show our results in Fig. 5. We obtain these results for case (i) GW170817 and all ten BBHs, and case (ii) GW170817 and only the five BBHs above (GW150914, GW151226, GW170608, GW170814, GW170818). While in the former case with all ten BBHs larger differences are seen, no significant differences with varying population parameters are observed in the latter case with only the five BBHs used in the main analysis. This demonstrates the robustness of our final result against the assumptions on the population distribution parameters, and further justifies our criterion of using only the "high in-catalog probability" BBHs. We would like to note that choosing a subset of detected events might itself introduce a selection bias due to a preference for nearby and/or loud sources. This effect is expected to be small compared to the current statistical uncertainties, and in the future, we expect to perform a thorough treatment marginalizing over these population assumptions.

5.2. *Luminosity weighting*

The results in the previous section assumed a weighting of galaxies by their luminosities in the B-band. Luminosities in the B-band are indicative of galaxies' star formation rates. The star formation rate of a galaxy might not correspond to its probability of hosting a binary merger. In absence of a robust astrophysical model of binary mergers, it may be more appropriate to weight galaxies by their total masses instead. Luminosities in the infra-red (K-band) are more indicative of the total masses of galaxies; however K-band luminosities are not present in catalogs like DES-Y1 and GWENS which we use and reliable extrapolation schemes are not available. In order to quantify the difference likely to be caused by alter-

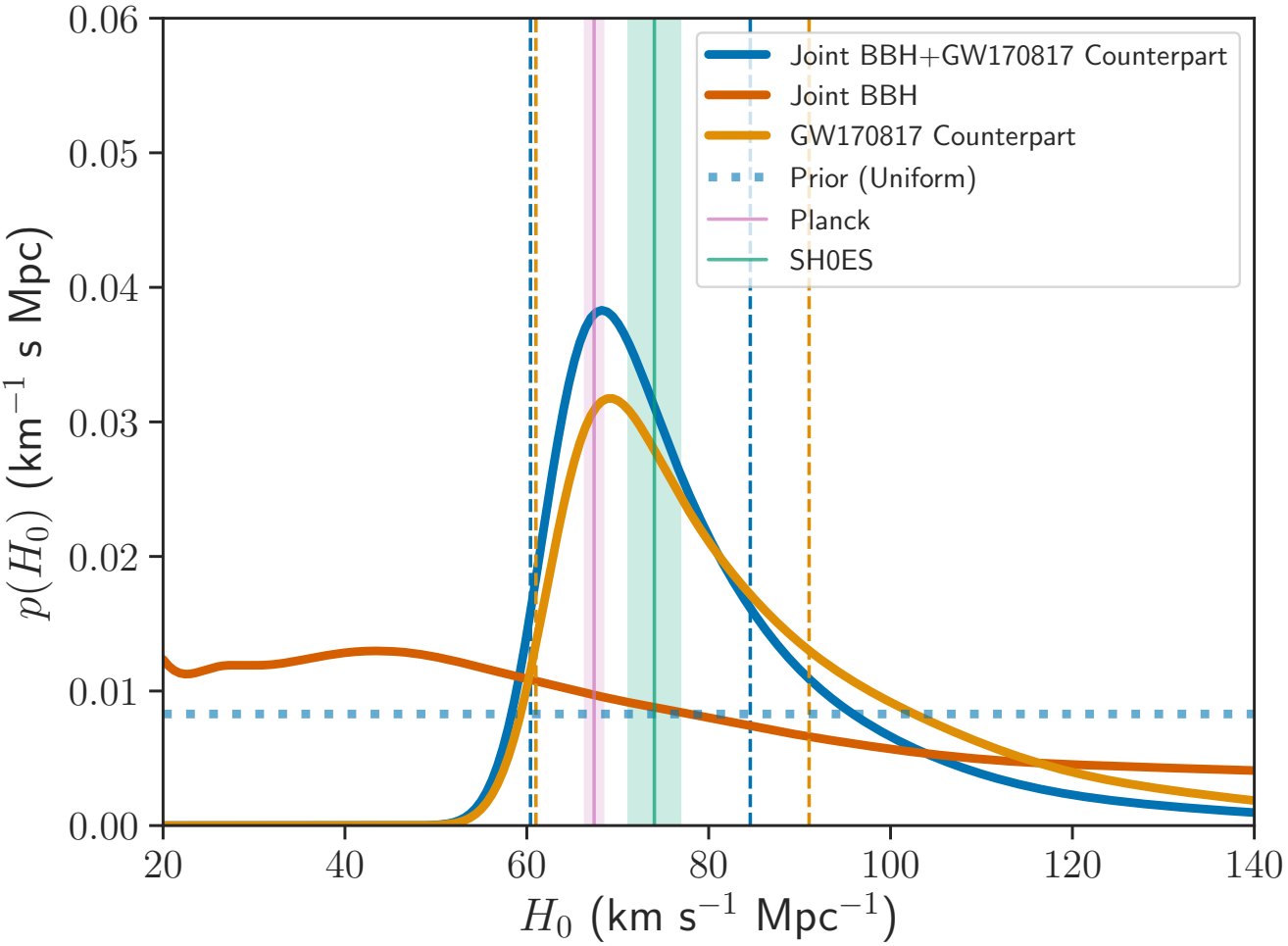

Figure 4. The gravitational-wave measurement of H_0 (dark blue) from the detections in the first two observing runs of Advanced LIGO and Virgo. The GW170817 estimate (orange) comes from the identification of its host galaxy NGC4993 (Abbott et al. 2017b). The additional contribution comes from binary black holes in association with appropriate galaxy catalogs; for GW170814 and GW170818 we use the DES-Y1 and GWENS galaxy catalogs respectively, while for GW150914, GW151226, and GW170608, we use the GLADE catalog. We do not use the other binary black holes for this result. The 68% maximum a-posteriori intervals are indicated with the vertical dashed lines. All results assume a prior on H_0 uniform in the interval [20, 140] km s^{-1} Mpc^{-1}(dotted blue). We also show the estimates of H_0 from CMB (Planck: Aghanim et al. 2018) and supernova experiments (SH0ES: Riess et al. 2016).

nate ways of weighting the galaxies, we repeat our analysis with no luminosity weighting. These results are shown in Fig. 6.

With uniform luminosity weights, we obtain a result on a joint binary black hole estimate which is essentially flat (thin orange line in Fig. 6). This can be understood as follows: 1) The out-of-catalog terms in Eq. (6) take into account the lack of galaxies beyond the apparent magnitude threshold $m_{\rm th}$ of the catalog in a uniform way. 2) The photometric redshift uncertainties calculation described in Section 3.4.1 performs the marginalization over the redshift uncertainty of each galaxy by effectively introducing more galaxies to wash out any artificial structure introduced by the photometric redshifts. These two effects make the galaxy catalog appear quite uniform, and with the lack of luminosity weights any remaining structure in the catalog is effectively washed out. With luminosity weights we give more probability to galaxies which are more luminous, retaining the structure of the catalog even after the addition of out-of-catalog terms and marginalization over photometric redshift uncertainties. This is also in agreement with our expectations from Fishbach et al. (2019) and Gray et al. (2019), where weighting by luminosities enhance the features in the posterior distribution coming from the galaxy catalog.

5.3. *Photometric measurement of redshift*

Systematic effects due to the photometric measurement of redshift are smaller than current statistical uncertainties. Using alternate Schechter function parameters, and choosing lu-

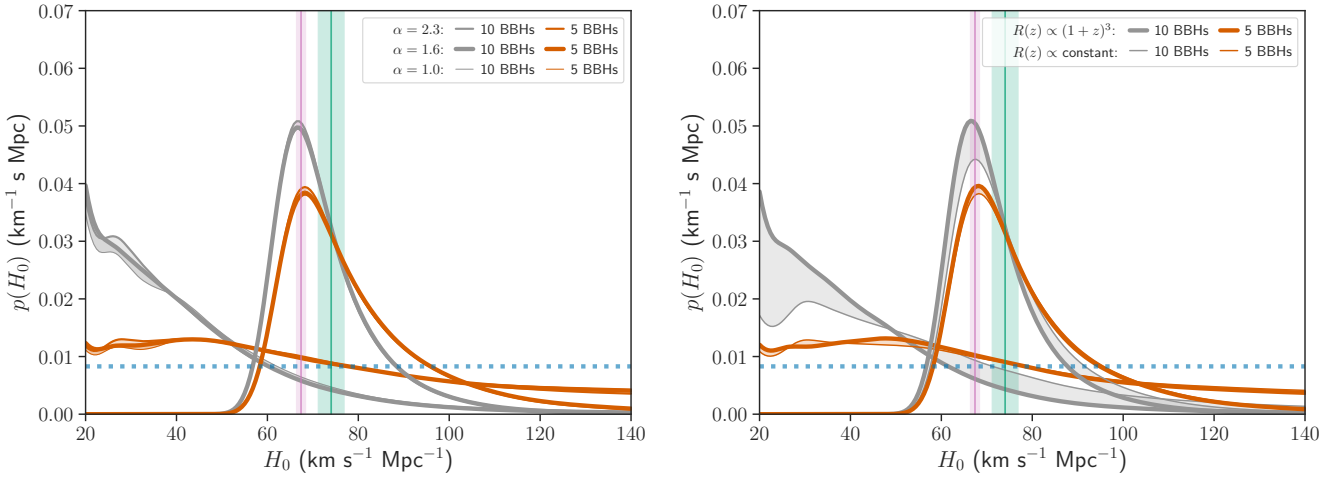

Figure 5. Sensitivity of the results to the mass distribution and the rate evolution model. *Left panel:* Variation of the results with three different choices of the power-law index for the mass distribution, $\alpha = 1.6$ (thick solid), $\alpha = 2.3$ (thin solid) and $\alpha = 1$ (thinner solid) assuming a constant intrinsic astrophysical merger rate, $R(z) =$ constant. *Right panel:* Variation of the results with two different choices for the rate evolution, $R(z) =$ constant (thick solid), and $R(z) \propto (1+z)^3$ (thin solid), for $\alpha = 1.6$. Both panels show combined estimates from all ten BBHs (gray) and only the five BBHs (GW150914, GW151226, GW170608, GW170414, GW170818) selected for our final results (orange). We also show how our final combined BNS + BBH result changes when either all ten or only five BBH events are considered. While there are larger variations when all ten detections are included, the variations are significantly smaller with only the five selected BBHs. This feature is more distinct for the rate evolution case where the two choices produce nearly identical estimates with only five BBHs (orange lines overlap in the right panel).

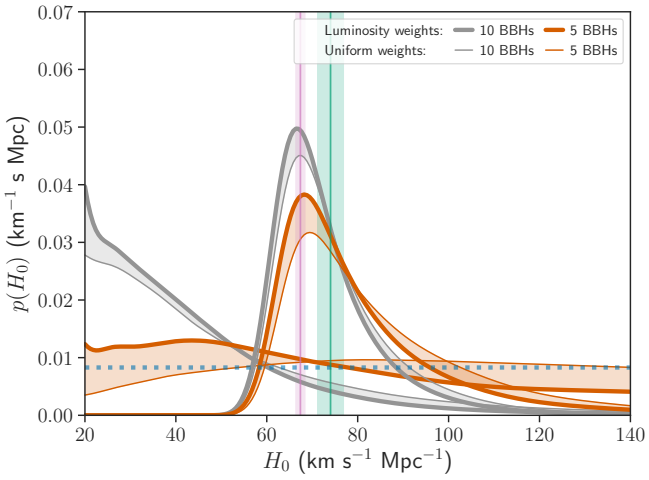

Figure 6. Sensitivity of the results to luminosity weighting. We show how the results vary when we weight the galaxies in the catalog by their B-band luminosity (thick solid) as well as with constant (uniform) weights (thin solid), both assuming a power-law index for the mass distribution, $\alpha = 1.6$ and constant intrinsic astrophysical merger rate, $R(z) =$ constant.

minosities allowed by our extrapolation scheme and redshift uncertainties in Section 3, we do not observe a significant difference in the results. For a more thorough treatment, and with an increasing number of detections, it will however become important to marginalize over the uncertainties in the choice of Schechter function parameters and other sources of error in the photometric EM measurement.

5.4. *Waveform models*

The posterior samples of Abbott et al. (2018b) used for the results in this paper have been obtained combining the results of gravitational waveform models which incorporate spin and precession effects to different extent (Husa et al. 2016; Khan et al. 2016; Hannam et al. 2014; Pan et al. 2014; Taracchini et al. 2014; Babak et al. 2017). These models are restricted to quasi-circular orbits (*i.e.*, they do not include orbital eccentricity) and neglect higher-order harmonics. Systematic differences in GW parameter estimation results with the employed waveform models constitute only a small fraction of the total uncertainty budget (see, *e.g.*, Abbott et al. 2016a, 2017c), and given the large statistical uncertainties, the ignored effects in waveform modeling are not expected to cause a difference to the current measurement of H_0. However cumulative systematic effects arising from limitations of waveform models will become increasingly important as the statistical uncertainties become smaller and, in particular, features that can lead to biases in the GW estimation of distance will need to be incorporated.

5.5. *Detector calibration*

An independent effect to be considered is the calibration of the GW detectors. Currently, the GW parameter estimation results are marginalized over the detector calibration uncertainties ($\lesssim 4\%$ in amplitude), which accounts for both the

statistical uncertainty and the systematic error correlated between detections (Abbott et al. 2018b). Both the statistical uncertainty and the systematic error in GW detector calibration are much smaller than the other measurement uncertainties, and thus negligible for H_0 estimates from a handful of detections that we have now or expect in the near future (Cahillane et al. 2017). However, the impact of correlated systematic calibration errors between detections will become relatively more important in the long term, with an increasing number of detections driving down the statistical uncertainties, and an improved understanding of other systematic effects that possibly govern our current uncertainty budget. Further quantitative study of the effect of correlated calibration uncertainties is ongoing.

6. CONCLUSION AND OUTLOOK

In this paper we have presented the first measurement of the Hubble constant using multiple GW observations. Our result reanalyzes and combines the posterior probability distribution obtained from the BNS event GW170817 using the redshift of the host galaxy inferred from the observed EM counterpart (Abbott et al. 2017b), along with constraints using galaxy catalogs for the BBH events observed by Advanced LIGO and Virgo in their first and second observing runs. We measure $H_0 = 68^{+14}_{-7}$ km s^{-1} Mpc^{-1} (68.3% highest density posterior interval with a flat-in-log prior). This result is mainly dominated by the information from GW170817 with its counterpart, but does show a modest improvement with the inclusion of the BBHs. The BBHs contribute both from associated galaxy catalogs as well as via their observed luminosity distance distribution. Since the latter contribution is sensitive to the assumptions on the mass distribution and rate evolution, we use for our final result only those BBHs for which the contribution comes significantly from galaxies present in the catalog. A more thorough treatment requires a marginalization over these unknown population parameters.

The contribution from events without counterparts is dominated by detections for which the galaxy catalogs are more complete. This highlights the importance of deeper surveys and of dedicated EM follow-up of sky regions following GW triggers for a better H_0 measurement. With numerous anticipated detections in the upcoming observing runs with improved detector sensitivities (Abbott et al. 2018c, 2016b,a, 2017a, 2018b,a), these results pave the road towards an era of precision multimessenger cosmology to be performed with a multitude of sources, including both neutron star and black hole mergers, with or without transient EM counterparts.

ACKNOWLEDGMENTS

The authors gratefully acknowledge the support of the United States National Science Foundation (NSF) for the construction and operation of the LIGO Laboratory and Advanced LIGO as well as the Science and Technology Facilities Council (STFC) of the United Kingdom, the Max-Planck-Society (MPS), and the State of Niedersachsen/Germany for support of the construction of Advanced LIGO and construction and operation of the GEO600 detector. Additional support for Advanced LIGO was provided by the Australian Research Council. The authors gratefully acknowledge the Italian Istituto Nazionale di Fisica Nucleare (INFN), the French Centre National de la Recherche Scientifique (CNRS) and the Foundation for Fundamental Research on Matter supported by the Netherlands Organisation for Scientific Research, for the construction and operation of the Virgo detector and the creation and support of the EGO consortium. The authors also gratefully acknowledge research support from these agencies as well as by the Council of Scientific and Industrial Research of India, the Department of Science and Technology, India, the Science & Engineering Research Board (SERB), India, the Ministry of Human Resource Development, India, the Spanish Agencia Estatal de Investigación, the Vicepresidència i Conselleria d'Innovació, Recerca i Turisme and the Conselleria d'Educació i Universitat del Govern de les Illes Balears, the Conselleria d'Educació, Investigació, Cultura i Esport de la Generalitat Valenciana, the National Science Centre of Poland, the Swiss National Science Foundation (SNSF), the Russian Foundation for Basic Research, the Russian Science Foundation, the European Commission, the European Regional Development Funds (ERDF), the Royal Society, the Scottish Funding Council, the Scottish Universities Physics Alliance, the Hungarian Scientific Research Fund (OTKA), the Lyon Institute of Origins (LIO), the Paris Île-de-France Region, the National Research, Development and Innovation Office Hungary (NKFIH), the National Research Foundation of Korea, Industry Canada and the Province of Ontario through the Ministry of Economic Development and Innovation, the Natural Science and Engineering Research Council Canada, the Canadian Institute for Advanced Research, the Brazilian Ministry of Science, Technology, Innovations, and Communications, the International Center for Theoretical Physics South American Institute for Fundamental Research (ICTP-SAIFR), the Research Grants Council of Hong Kong, the National Natural Science Foundation of China (NSFC), the Leverhulme Trust, the Research Corporation, the Ministry of Science and Technology (MOST), Taiwan and the Kavli Foundation. The authors gratefully acknowledge the support of the NSF, STFC, INFN and CNRS for provision of computational resources.

REFERENCES

Abbott, B., et al. 2017a, Phys. Rev. Lett., 119, 161101

Abbott, B. P., et al. 2016a, Phys. Rev., X6, 041015, [erratum: Phys. Rev.X8,no.3,039903(2018)]

—. 2016b, Astrophys. J., 833, L1

—. 2017b, Nature, 551, 85

—. 2017c, Class. Quant. Grav., 34, 104002

—. 2018a, arXiv:1811.12940 [astro-ph.HE]

—. 2018b, arXiv:1811.12907 [astro-ph.HE]

—. 2018c, Living Rev. Rel., 21, 3

Abbott, T. M. C., et al. 2018d, Astrophys. J. Suppl., 239, 18

Aghanim, N., et al. 2018, arXiv:1807.06209 [astro-ph.CO]

Babak, S., Taracchini, A., & Buonanno, A. 2017, Phys. Rev., D95, 024010

Beck, R., Dobos, L., Budavári, T., Szalay, A. S., & Csabai, I. 2016, MNRAS, 460, 1371

Birrer, S., et al. 2019, Mon. Not. Roy. Astron. Soc., 484, 4726

Caditz, D., & Petrosian, V. 1989, ApJL, 337, L65

Cahillane, C., Betzwieser, J., Brown, D. A., et al. 2017, Phys. Rev. D, 96, 102001

Carrick, J., Turnbull, S. J., Lavaux, G., & Hudson, M. J. 2015, Mon. Not. Roy. Astron. Soc., 450, 317

Chen, H.-Y., Fishbach, M., & Holz, D. E. 2018, Nature, 562, 545

Cook, D. O., Dale, D. A., Johnson, B. D., et al. 2014, MNRAS, 445, 890

De Vicente, J., Sánchez, E., & Sevilla-Noarbe, I. 2016, Mon. Not. Roy. Astron. Soc., 459, 3078

Del Pozzo, W. 2012, Phys. Rev., D86, 043011

Drlica-Wagner, A., et al. 2018, Astrophys. J. Suppl., 235, 33

Dálya, G., Galgóczi, G., Dobos, L., et al. 2018, Mon. Not. Roy. Astron. Soc., 479, 2374

Feeney, S. M., Peiris, H. V., Williamson, A. R., et al. 2019, Phys. Rev. Lett., 122, 061105

Fishbach, M., Gray, R., Hernandez, I. M., Qi, H., & Sur, A. 2019, Astrophys. J., 871, L13

Fishbach, M., Holz, D. E., & Farr, W. M. 2018, Astrophys. J., 863, L41

Gehrels, N., Cannizzo, J. K., Kanner, J., et al. 2016, Astrophys. J., 820, 136

Gray, R., et al. 2019, https://dcc.ligo.org/P1900017, TBD

Hannam, M., Schmidt, P., Bohé, A., et al. 2014, Phys. Rev. Lett., 113, 151101

Hinshaw, G., Weiland, J. L., Hill, R. S., et al. 2009, ApJS, 180, 225

Holz, D. E., & Hughes, S. A. 2005, Astrophys. J., 629, 15

Husa, S., Khan, S., Hannam, M., et al. 2016, Phys. Rev., D93, 044006

Khan, S., Husa, S., Hannam, M., et al. 2016, Phys. Rev., D93, 044007

Kiziltan, B., Kottas, A., & Thorsett, S. E. 2010, arXiv:1011.4291 [astro-ph.GA]

Macaulay, E., et al. 2019, Mon. Not. Roy. Astron. Soc., 486, 2184

MacLeod, C. L., & Hogan, C. J. 2008, Phys. Rev., D77, 043512

Madgwick, D. S., Lahav, O., Baldry, I. K., et al. 2002, MNRAS, 333, 133

Mandel, I., Farr, W. M., & Gair, J. R. 2019, Mon. Not. Roy. Astron. Soc., 486, 1086

Messenger, C., & Read, J. 2012, Phys. Rev. Lett., 108, 091101

Mortlock, D. J., Feeney, S. M., Peiris, H. V., Williamson, A. R., & Nissanke, S. M. 2018, arXiv:1811.11723 [astro-ph.CO]

Nair, R., Bose, S., & Saini, T. D. 2018, Phys. Rev., D98, 023502

Nissanke, S., Holz, D. E., Dalal, N., et al. 2013, arXiv:1307.2638 [astro-ph.CO]

Nissanke, S., Holz, D. E., Hughes, S. A., Dalal, N., & Sievers, J. L. 2010, Astrophys. J., 725, 496

Pan, Y., Buonanno, A., Taracchini, A., et al. 2014, Phys. Rev., D89, 084006

Rahman, M., Nissanke, S., Williamson, A., et al. 2019, (in preparation)

Riess, A. G., Casertano, S., Yuan, W., Macri, L. M., & Scolnic, D. 2019, Astrophys. J., 876, 85

Riess, A. G., et al. 2016, Astrophys. J., 826, 56

Sadeh, I., Abdalla, F. B., & Lahav, O. 2016, Publ. Astron. Soc. Pac., 128, 104502

Sathyaprakash, B. S., Schutz, B. F., & Van Den Broeck, C. 2010, Class. Quant. Grav., 27, 215006

Saunders, W., Rowan-Robinson, M., Lawrence, A., et al. 1990, Monthly Notices of the Royal Astronomical Society, 242, 318

Schutz, B. F. 1986, Nature, 323, 310

Soares-Santos, M., et al. 2019, Astrophys. J., 876, L7

Taracchini, A., et al. 2014, Phys. Rev., D89, 061502

Taylor, S. R., & Gair, J. R. 2012, Phys. Rev., D86, 023502

Wolf, C., Dye, S., Kleinheinrich, M., et al. 2001, Astron. Astrophys., 377, 442